Studies on the development of image analysis for plant research

Kato, Seiji

(Degree)
博士（学術）

(Date of Degree)
2014-07-18

(Date of Publication)
2015-07-01

(Resource Type)
doctoral thesis

(Report Number)
乙第3257号

(URL)
https://hdl.handle.net/20.500.14094/D2003257

Studies on the Development of Image Analysis for Plant Research

Seiji Kato

Contents

Chapter 1.

Introduction

It is estimated that visual cues account for about 80 % of external stimuli that humans receive from their surroundings [1]. Visual information is also important in plant science and researches. However, because the data for describing visual information are usually extensive and difficult to understand, scientists have continually sought ways in which visual information can be represented by converting it to numerical values and measurements such as length, angle and area. Certain visual information, like color depth, is particularly difficult to evaluate without a subjective scale. Consequently, analyses of visual information have frequently annoyed scientists in trouble. Only expert researchers were able to evaluate them through naked eyes. Therefore objective evaluation method was demanded.

Computer technology has been developed rapidly since the late 20th century and computers have become very helpful, sometimes even indispensable, tools for research in the field of image analysis, because they can be used to process visual information objectively. In the past, because of high cost and need for dedicated instruments, only a few researchers had access to such systems for digital image analysis [2-4]. Image analysis is now both popular and necessary for a variety of research activities and it is used widely from the micro-field to the macrofield in the plants study. In the fundamental research field, as the micro example, there is chromosome analysis by the microscopy [5]. And, as the macroexample, distribution of the vegetation is analyzed using the remote sensing with the satellite image [6]. Moreover, it came to be used widely in the applied science field of the agriculture business such as the discrimination of the damaged rice grain [7].

Chromosome is a structure containing DNA-coded genes and histone proteins. It relates to genetics and heredity deeply. Chromosome has specific, reiterated sequence of centromere [8-11] and the telomere [12-14] relating the chromosomal conformations. By the positions and the locus of these repeated sequences and DNA markers, respectively, relationship and differentiation of the species would be clear. Moreover, it becomes able to improve plant breeding drastically by positioning specific gene sequences on chromosomes. Genome projects were completed with rice [15] and the Arabidopsis [16], and the result has a big influence on the breeding of the plant, and

there are the gene markers obtained from linkage maps. The marker breeding using the gene markers can greatly shorten a breeding term to be able to select it before phenotypic expressions [17-20]. Development of chromosome maps is important for understanding genetic arrangements and diversity. It is thought that detailed chromosome maps contribute to prevention and cure of hereditary diseases, and creation of superior field crops.

Chromosome map is shown as chromosomal pattern diagram called 'idiogram'. The initial idiograms in early days is reproducing chromosomal characters caught by naked eyes as illustrations. The extraction of features from the chromosome image was common to today's image analyzing method. Now, chromosomal images were recorded by a microscope imager. By the employment of the cooled CCD camera to detect a very small amount of light, the digitization of the chromosome image progressed rapidly, and the affinity with the image analysis became higher. Additionally, Fluorescence *in situ* hybridization (FISH) which labeled fluorescent dyes to genes was developed [21]. Reiterated sequences were positioned on chromosomes with a lot of kinds such as centromeres [8, 9, 22, 23], telomeres [13, 24, 25], rDNAs [26-32] by FISH. The epigenetic phenomenon in relation to the gene activation and inactivation is one of important factors in genomics [33-36]. Histone modification in chromosomes or nucleus is an interesting phenomenon, and the visualization technology by the immunostaining is developed [37-39]. The image analysis contributes the chromosome analysis which is important tool of biological research.

There is the long history of chromosome image analysis in plants. Chromosome mapping was developed by gene loci and the number of the band appeared on a chromosome by differential staining technique such as G-band or C-band [40], and the image analysis technology was progressed mainly with human chromosomes [41, 42]. Detailed bands were not obtained in plants, and particularly clear bands were not revealed in small chromosomes. In the 1980s, Fukui *et al.* [5] developed Chromosome Image Analyzing System (CHIAS), and the development of the chromosome map (quantitative idiogram) by the condensation pattern was enabled. An accurate chromosome map was developed in the small plant chromosome which had

difficulty in identification. However, the image analysis technology was available only to limited researchers, because expensive exclusive image-processing equipment was necessary.

Not only for chromosome analysis as the example at the micro-level, image analysis is also useful for estimation and evaluation of plant shape. It has been used for the analysis such as the shapes of seeds and the leaf from the late 1980s [43]. As an example of the image analyses of, an evaluation of plant shape analysis of the soybean (*Glycine max*) was reported in the 1990s [44]. The skillful breeders with few quantitative data selected the good plant shape of soybean only empirically. Features of plant shape were able to be extracted by the transduction of the image analysis, but were not able to expect the spread in plant researches, because an exclusive image-processing unit was necessary either. In addition, the situation was different from microscope photography, and there was little tool of the digitization, and there was a limit to resolution of the video camera. Therefore, these devices were not suitable for the image analysis As an example of the flowers of the image analysis about spray formation of chrysanthemum was reported, but exclusive image processing unit and video camera was required [45]. Development of the software was necessary about the relatively simple measurement of the leaf area [46]. These limitations were eliminated by the rapidly development of the computer, and a process of the image information became easy by a combination of digital camera and personal computer. Resolving these problems, a program with better human interface and lower cost is required for the application of the variable plants materials.

To resolve these research problems, I investigated the image analysis method using several kinds of plant material with regard to plant chromosomes and appearance shapes. For effective studies of plant chromosome, it is important to understand total genomics by the combination of chromosome image analysis and FISH method. The present study is to establish and confirm the effectiveness of these methods. An image analysis method was applied for the evaluation of flowering degree of Christmas Erica to express more effectively of the plant figures. Although it was not practical to measure the number of the flowers, in the case of Christmas Erica having several thousands of

flowers per pot, quantifying area of white flowers became possible.

The purposes of the study are: firstly developed such of programs for image analyses of plant chromosomes, which work personal computers without using exclusive image processing equipment, secondly, development of chromosome maps which were significant biologically in several kinds of plants, and thirdly, evaluation of the pot flower using the developed program.

In Chapter 2, I describe of the development of CHIAS version III that is working only on personal computer and demonstrate compatibility with conventional CHIAS. In Chapter 3, I describe the development of a chromosome map of all chromosomes of sugarcane (*Saccharum spontaneum*), what is gramineous autopolyploidy and is adequate as an analysis example using CHIAS III and FISH method. In Chapter 4, development of a high-resolution pachytene chromosome map of chromosome 9 using meiotic cells of rice (*Oryza sativa*) is described. In this chapter, a technology for clarifying chromosome conformation called "chromomere" which appears in meiotic pachytene chromosomes more clearly is described. In Chapter 5, development of chromosome image analysis system CHIAS IV is described. CHIAS IV incorporates automation of complicated process of CHIAS III to develop a chromosome map quickly and an example is shown for the development of a chromosome map in red clover. In Chapter 6, development of the quality evaluation methods is shown using image analysis of Christmas Erica which is the special product of Yamanashi prefecture. The bush is trained in the style of a fir tree covered with snow. Christmas Erica is spread in the market with high prices in Yamanashi prefecture. An objective quality evaluation standard is needed to keep price higher over the long term, because the maintenance of quality became important. An objective index for quality evaluation was developed by measuring area of flowers using image analysis.

Chapter 2.

Condensation pattern (CP) analysis of plant chromosomes by an Improved chromosome image analysing system, CHIAS III

2.1 Introduction

Plant chromosomes are categorized into two types by their sizes, such as the large type (L-type) typically shown in lily, rye, and barley chromosomes, in which clear banding patterns appear by chemical treatments. The small type (S-type) is represented by rice, soybean and *Brassica* chromosomes, in which there are no bands, or a few bands appear in limited regions of the chromosomes such as centromeric positions [47, 48]. Instead of lacking a band that serves as a good landmark to identify chromosomes, the S-type chromosomes in plant show a natural, uneven staining pattern on their chromosomes, especially at the prometaphase stage, which has been noticed by many plant cytologists for years (e.g., [49]).

The uneven staining pattern has been found to correspond to uneven condensation of the chromatin fiber in a chromosome during the prometaphase. The condensation pattern (CP) has been found to be effective for identifying small plant chromosomes based on the complete identification of all the rice chromosomes [50]. In fact, more than 90 % of rice chromosomes could be automatically identified by using only the CP or the numerical data of the CP [51] , clearly demonstrating that the CP is a representative image parameter of chromosome morphology.

Two image analyzing systems have been used for the CP analysis: the first-generation chromosome image analyzing system, CHIAS, with CP/M operating system and with the image file format specific to the CHIAS [5], and the second- generation system, CHIAS II, with MS/DOS operating system and with the image files common to most of the other systems [52]. If an imaging system, a universal system without specific hardware and software, could be constructed, then the analysis of small plant chromosome could advance further.

Against this background, I developed the third-generation chromosome image analyzing system, CHIAS III, which is anticipated to broaden availability of image analysis methods in chromosome research because CHIAS III consists of an ordinary personal computer, and does not depend on specific imaging software that runs on limited systems but uses public domain software available via the Internet. Furthermore, consistency of the data between those obtained with CHIAS III and the previous

systems was also experimentally confirmed.

2.2 Materials and methods

2.2.1 Source of chromosome image and system implementation

Chromosome samples of a haploid line of a wild sugarcane plant, *Saccharum spontaneum* L. (AP301, $2n=4x=32$ [53]) were prepared using the enzymatic maceration and air-drying (EMA) method [48] and were stained with a 2% Giemsa solution. Chromosome images were photographed through Axiophot (Zeiss) with an oil immersion x100 objective lens. A chromosome spread without cytoplasmic debris and overlapping chromosomes was selected and used as a model spread for the CP analysis.

The chromosome spread recorded on 35-mm negative film (ISO 32, Neopan F, Fujifilm) was digitized by a film scanner (1,350 dpi, Polascan 35, Polaroid) and stored as a 781 kbyte TIFF file (Tagged image file format, 1,000 × 800 pixels size, 8 bit gray steps/pixel) by using a version of Adobe PhotoShop LE (Adobe Systems) on the hard disk of a personal computer; Power Macintosh (7100/66AV, Apple) with a hard disk memory (500 Mbyte), RAM (72 Mbyte), a color monitor (8bit × 3 colors). A silver halide color printer (Pictrography 4000, Fujifilm) was used for printing the results.

The same chromosome images printed on photographic paper using the same negative film was captured in CHIAS II, which runs on a universal image analyzer (IBAS or VIDAS, Zeiss/Kontron), via a monochrome CCD (charge-coupled device) camera (XC-77CE, Sony) on a copy stand.

2.2.2 Software for CP analysis

The CP analysis was performed on a Macintosh mainly using the public domain NIH Image program (written by Wayne Rasband at the US National Institute of Health and available from the Internet by anonymous ftp from zippy.nimh.nih. (Windows version can be downloaded from http://www.scioncorp.com/). A rank operation filter (median filter with a 5 × 5 filter matrix size, PhotoShop plug-in filter compatible with the NIH Image), Copyright 1992 by John C. and J. Christian Russ, was

acquired via the Internet by russ@mat.mte.ncsu.edu. A spread-sheet program, Microsoft Excel (Ver. 5.0, Microsoft) was used for calculation of averaged CPs or standard CPs to develop idiograms.

A new command, Measure CP, for simultaneous acquisition of length of a broken line and corresponding gray values was programmed using a Pascal-like NIH Image macro language. Measure CP was used throughout the CP analysis. A new look-up table, Chromoart K01, for pseudo-coloration of chromosome images was also programmed to enhance human visual sense for the detection of the CP. More information about the software including the look-up table, command, macros, and the tutorial can be obtained via the Internet (http://www2.kobe-u.ac.jp/~ohmido/cl/chiasIII/index.htm). A stepwise written manual for all the procedures for the CP analysis with the CHIAS III is also available [54].

The CP analysis using CHIAS II was simultaneously carried out for the photographic image in the same chromosomal spread by the method reported previously [55]. All the numerical data of the condensation pattern obtained from the chromosomes within the spread either with the CHIAS II or CHIAS III were compared and a conversion table for gray values between the two systems was developed by using Microsoft Excel.

2.3 Results

Figure 2-1 shows a digital image of a prometaphase chromosomal spread with 32 chromosomes in a haploid, wild sugarcane plant. Each of eight homologous groups has four chromosomes. The chromosomes showed uneven staining patterns or condensation patterns along the chromosomes. All the chromosomes were visually classified in each of eight homologous groups by microscopic examination of the CP before the CP analysis using CHIAS III. The photographic image of the same chromosomal spread was also subjected to the CP analysis with the CHIAS II.

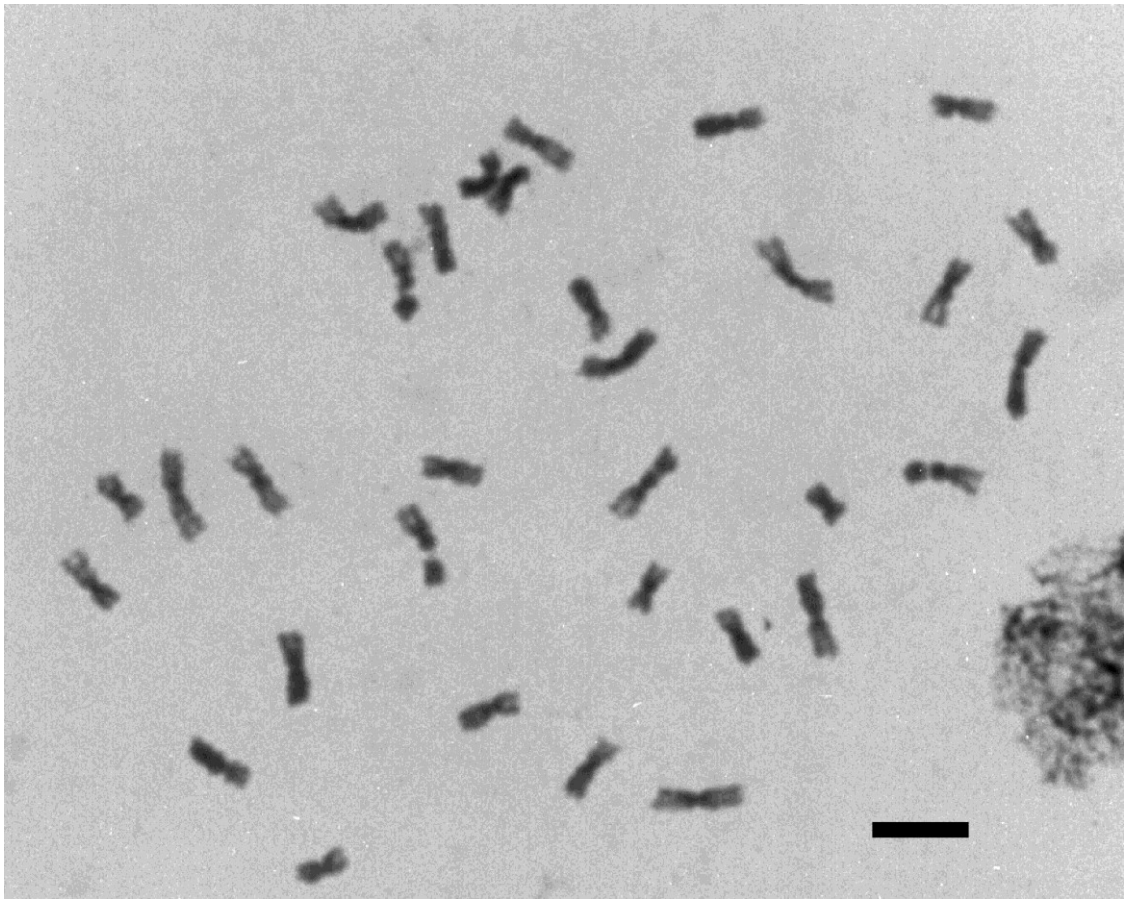

Figure 2-1. Prometaphase chromosome spread derived from anther culture of a wild sugarcane, *S. spontaneum* L. (2*n*=4*x*=32). Bar = 5 um.

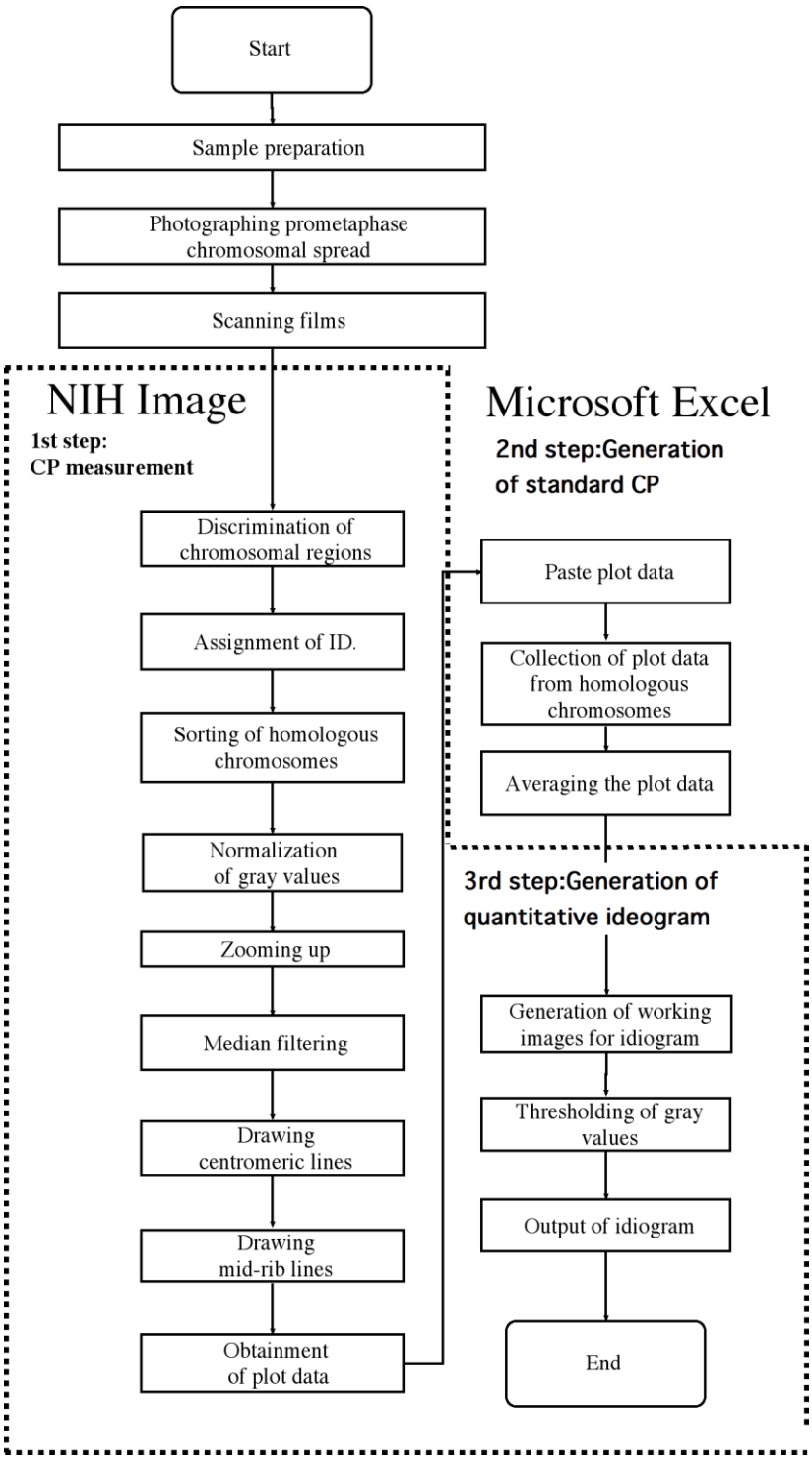

Figure 2-2. Flow chart of the CP analysis showing three major steps of CP measurement, generation of the standard CP and generation of quantitative idiogram.

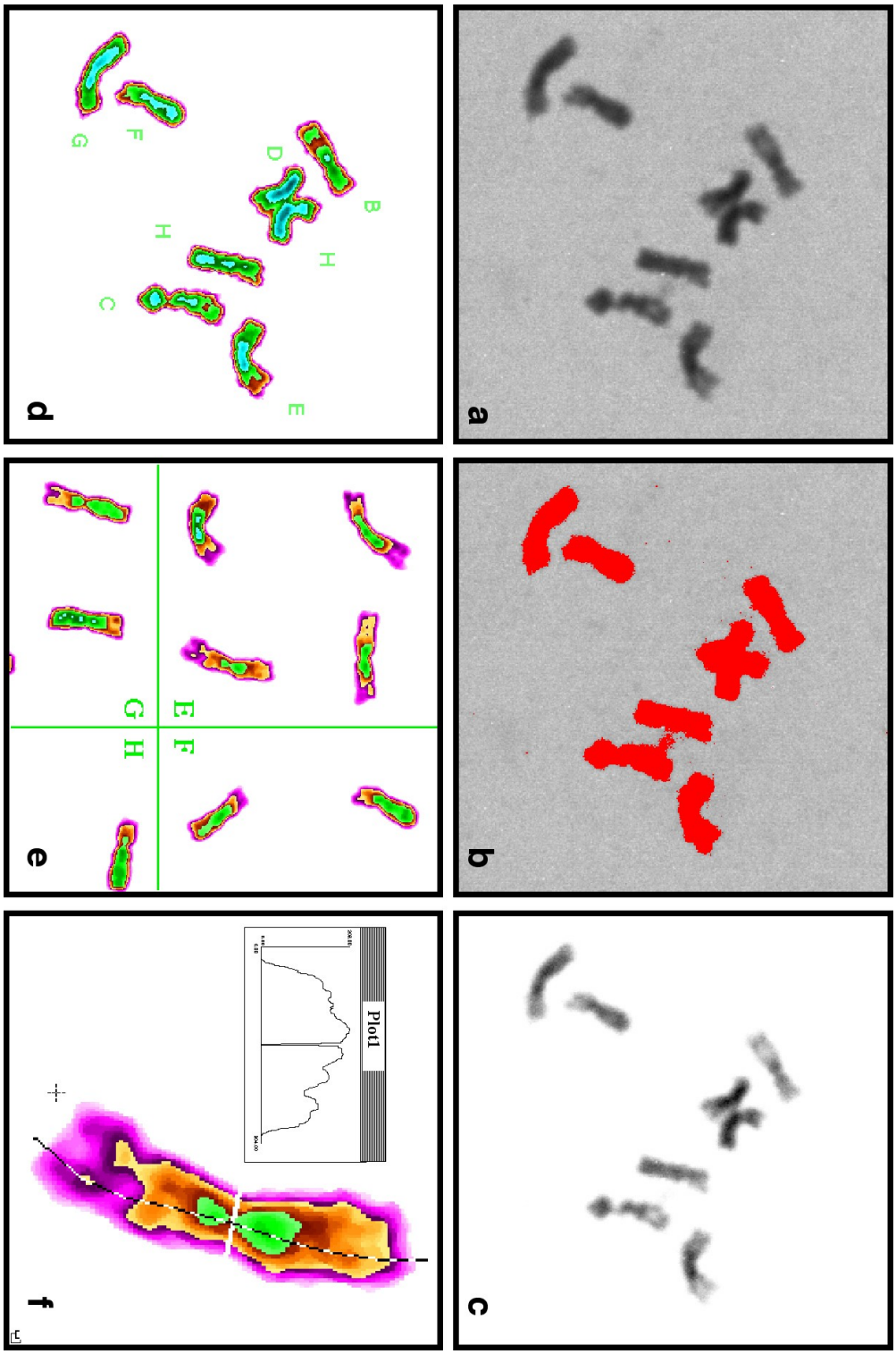

Figure 2-3. Representative steps of the image manipulation for CP analysis. The details are described in the text.

Figures 2-2 and 2-3 show a flow chart of the CP analysis and representative steps of the image manipulation for the CP analysis by using CHIAS III. The flow chart was divided into three major steps. First, chromosome images digitized by a film scanner were digitally pretreated before the measurement of the numerical data of the CP from each of 32 chromosomes. Figure 2-3a shows a captured area depicting eight chromosomes out of the 32 chromosomes in the 781-kbyte image; Figure 2-3b-f shows the same chromosomes. The chromosomal regions were discriminated from the background field by thresholding the gray level at the gray value, 102. The foreground chromosome images painted in red were recovered as the chromosomal regions (Figure 2-3b) and the chromosome images without background noises were obtained by elimination of the background field (Figure 2-3c).

Alphabetical identification from A to H indicating one of eight homologous groups of *S. spontaneum* was assigned according to the visual identification of the CP in advance of the acquisition of the digital data of the CP for each of the 32 chromosomes pseudo-colored by a look-up table, Chromoart K01 (Figure 2-3d). Then four homologous chromosomes with the same identification were collected together into one of the eight subpanels (a-h) in a homologous chromosome gallery using the commands Cut and Paste. Figure 2-3e shows a captured area depicting part of four subpanels of e-h in the homologous chromosome gallery. After cutting and pasting all the chromosomes into each of eight subpanels, the minimum gray value, 88, and maximum gray value, 229 were measured, and they were normalized or extended to their respective gray values 1 and 254 by application of the normalization digital filter. Gray values of all the pixels of each chromosome were allocated to the new, broadened range of the gray values.

Figure 2-4 depicts the homologous chromosome gallery with eight subpanels of homologous groups from a to h in which four chromosomes were allocated. The homologous chromosomes were visually checked again within each panel for the chromosome morphology, CP and staining condition, and necessary replacement of chromosomes between homologous groups or change in assignment of short and long arms was carried out as requested.

The targeted chromosome for CP measurement was first zoomed up and a median filter with a 5 × 5 pixel matrix size was then applied to alleviate the zooming up effect to the chromosome image (Figure 2-3f). A broken line tracing a mid-rib of a chromatid was interactively drawn, and the gray values under the line were automatically measured after the identification of a centromeric line at the primary constriction. Allocation of different colors by the look-up table was carried out to increase the discrimination as required. A density profile obtained at the mid-rib line of the enlarged chromosome was plotted in a subset window (Figure 2-3f). When the density profile was suitable by visual inspection, the plotted data were written in the memory of the Macintosh.

Second, the plotted data of all the CPs were copied to the spread sheet of Microsoft Excel. The length in pixels of respective short and long arms was averaged over eight chromatid mid-rib lines from four homologous chromosomes, and the corresponding gray value for each pixel was calculated. The averaged minimum and maximum gray values over the eight density profiles or CPs were calculated. The gray values of the eight profiles or CPs were again normalized by replacing the averaged minimum and maximum gray values as the new minimum and maximum values of each CP. Then an averaged density profile or standard CP (stCP) was generated with the averaged length of eight homologous chromatids and corresponding gray values. Fractional gray levels resulting from the averaging were rounded to the nearest integer. The two conventional parameters of relative length and arm ratio were also obtained by using the numerical data from the stCP.

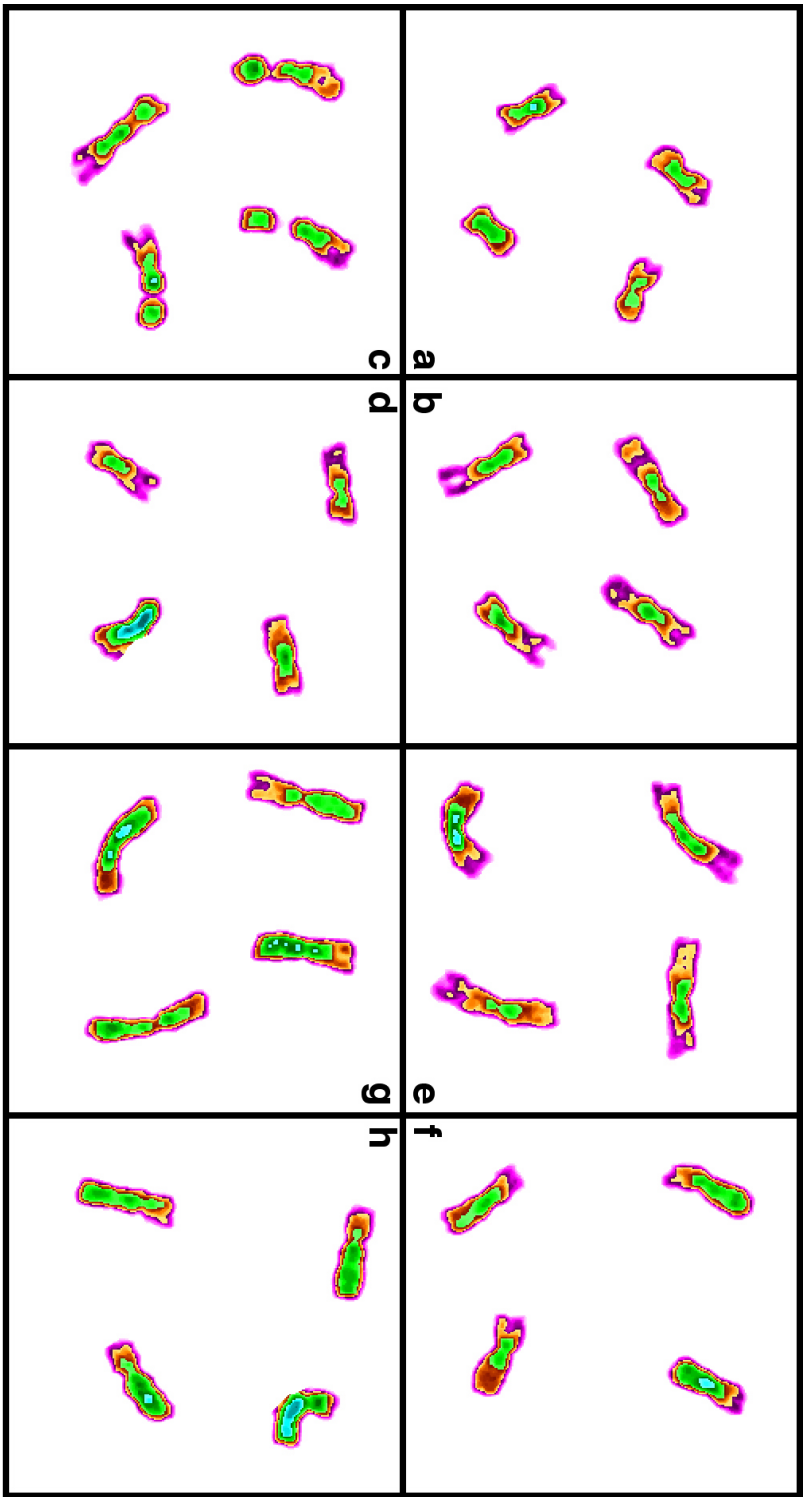

Figure 2-4. Homologous chromosome gallery of *S. spontaneum* L. Four homologous chromosomes are included in each of subpanels.

Figure 2-5a shows two stCPs of chromosome E generated both by CHIAS II and by CHIAS III. The gray values of the stCP obtained with CHIAS III were invert in Figure 2-5a because allocation of 0-255 gray values to black and white is different between CHIAS II and CHIAS III. Although two stCPs were different along the chromosomes in their averaged gray values, the general patterns between the two stCPs were quite similar to each other. Similarity in the patterns was recognized all over the eight stCPs. The coefficient of correlation was r^2=0.998 between the 1,332 pair of the gray values at the corresponding pixels of all the eight stCPs obtained using CHIAS II and CHIAS III. A quadratic conversion equation between the two gray values obtained with CHIAS II and CHIAS III was also formulated (Figure 2-5b).

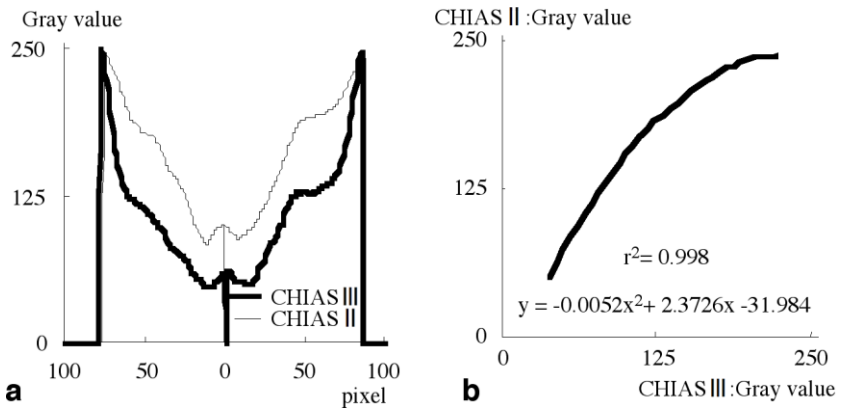

Figure 2-5. Comparison of the two standard CPs of chromosome E obtained with the CHIAS II and III.

Third, a quantitative chromosome map or idiogram of *S. spontaneum* was developed. Figure 2-6 shows representative karyotypes selected among four homologous chromosomes, stCPs averaged by four homologous chromosomes, density distribution bars or graygrams based on the stCPs, and idiograms. Thresholding stCPs at two gray values generated idiograms based on eight chromatids of a single chromosomal spread. The upper border (gray value=125) was fixed for all the cases and corresponded to the border between gray and white bars in the idiogram. The border corresponds to the visual border of condensed and dispersed regions of *S. spontaneum* chromosomes as in the case of rice chromosomes. The lower borders (gray values 64, 80, 93 and 96) between gray and black bars of the idiogram were set individually to represent the morphological features, such as the tertiary constrictions, visually detected on the individual chromosomes. Although the gray values of the lower borders thus depended on the individual chromosomes when only one chromosomal spread was used, the gray values of the lower borders could be unified or at least decreased in their number when the data were collected from a sufficient number of chromosomal spreads.

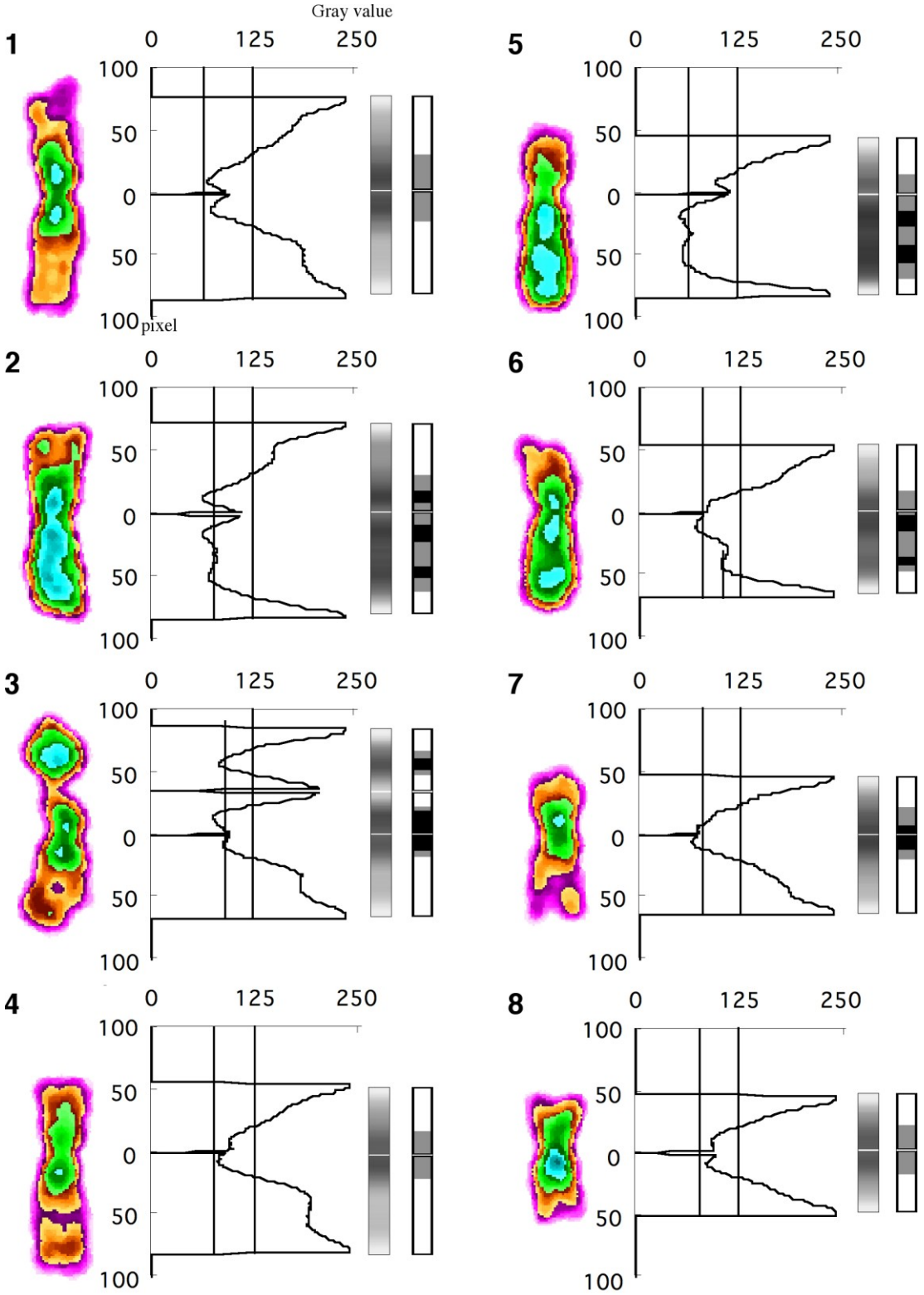

Figure 2-6. Karyotype, standard CP, graygram and idiogram for all the eight homologous chromosomes of *S. spontaneum* L.

2.4 Discussion

Computerized chromosome analyses began mainly by analyzing mammal chromosomes during the 1960's [56, 57]. Several advances both in the theoretical and in the applied disciplines have now made it possible to develop a variety of automated systems that can be used for diagnostic purposes [58-60]. Although comprehensive computerized analysis systems for plants, CHIAS I and II, were developed [5, 52], their main frames, specific image analyzers, delimited the usefulness of the systems.

The advantage of CHIAS III is that the system uses an ordinary personal computer with some common peripheral devices such as a color monitor, film scanner, color printer, etc. The main software can be obtained commercially and via the Internet. The necessary software specific to the CP analysis and generation of the idiogram has been programmed and can be obtained via the Internet. As a result, quantification of the CP appearing specifically at the mitotic prometaphase of small plant chromosomes can be satisfactorily achieved using CHIAS III.

The chromosome image analyzing system, CHIAS II, which uses a universal image analyzer and has already been developed and practically used, is a convenient system for the CP analysis with all the necessary components for the image analysis [52]. The effectiveness of the CP analysis with the CHIAS II has already been proved in previous studies [55, 61]. The data obtained with both CHIAS II and CHIAS III are also consistent based on the comparison between the gray values of the 1,332 pixels consisting of all the eight stCPs (Figure 2-5b).

The main difference in the stCPs obtained with the two systems lies in the relative gray values of the pixels but not in the pattern of density profiles. This fact also strongly suggested that the data obtained by the two systems are basically the same. The relative dynamic range of the gray values was usually higher in the CHIAS III than in CHIAS II (Figure 2-5a). It is, however, suggested that the differences are mainly caused by the setting conditions of input devices, the CCD camera and film scanner but not by the differences in the main systems. Thus standardization of conditions for image input among input devices will be necessary, although it may be not easily attained because of rapid development and changing models of computer-related equipment.

The validity of the condensation pattern at the prometaphase for the identification of small plant chromosomes has been reported by several cytologists for years. Hu [49] indicated the effectiveness of the condensation pattern in identifying 12 small rice chromosomes and classified them into eight types. Kurata and Omura [62] showed that the identification of rice chromosomes based on the condensation pattern could be achieved in conjunction with enzymatic maceration and flame-drying methods. The effectiveness of the condensation pattern was unequivocally verified by the introduction of an imaging method to characterize the condensation patterns of 12 rice chromosomes [50].

Several quantitative chromosome maps or idiograms based on the condensation pattern have also been developed using CHIAS I and II [50, 61] . Development of an idiogram requires a sufficient number of good chromosome spreads. Only one chromosome spread was used to generate a quantitative chromosome map as a model case in this paper. The analysis can be repeated for a sufficient number of spreads to develop a stable idiogram with fixed lower and upper thresholds in the gray levels for graygrams. In this regard, omission of the chromosome spreads that are statistically significantly different in total chromosome length is indispensable for avoiding contamination of the chromosomal spreads at the different mitotic stages.

I have described here an imaging method for analyzing chromosome morphology, especially density distribution, by a system using ordinary computing equipment and public domain software. It is anticipated that objective analysis of the condensation patterns will make significant progress and that a quantitative chromosome map that is the basis of many biological studies will be developed, even for small chromosomes in plants.

Chapter 3.

Quantitative chromosome map of the polyploid *Saccharum spontaneum* by multicolor fluorescence *in situ* hybridization and imaging methods

3.1 Introduction

Polyploidy is particularly prominent among angiosperm plants. It is estimated that 30 % to 35 % of the known species are polyploid [63]. Almost 75 % of the species in Gramineae are polyploid [64]. Polyploids typically show a wider range of ecological tolerances [64], and thus frequently occupy niches and habitats that cannot be occupied by their diploid relatives.

The Gramineae, or grass family, is one of the largest and most important families of flowering plants; according to Gould [65], it contains about 600 genera and 7500 species. This makes it the fifth largest family in number of species in the plant kingdom, but in terms of use by humans it is by far the most important. The Gramineae contains cereals such as wheat, rice, maize, barley, grain sorghum, and pearl millet, most of the forage and concentrated feeds consumed by domestic animals, and the world's most important source of sucrose, sugarcane.

Sugarcane is a large grass of the genus *Saccharum*. Polyploidy is recognized as extensive in *Saccharum.* In fact, there is no known diploid form in this genus. Although there is agreement about the polyploid state of *Saccharum*, until recently neither the level nor the type of polyploidy, i.e. either autopolyploidy or allopolyploidy, was known. Aneuploidy is common and is usually associated with hybridization between ploidy levels. Understanding evolution in *Saccharum* is complicated by natural hybridization across related genera such as *Erianthus*, *Miscanthus*, *Sclerostachya*, and *Narenga*. In addition, the taxonomy of the genus *Sccharum* has proven difficult because extensive hybridization and aneuploidy have blurred boundaries between genera and species. It is generally accepted that *Saccharum* contains three cultivated species (*S. officinarum* L., $2n$=80; *S. sinense* Roxb., $2n$=110-120; *S. barberi* Jesw., $2n$=82-124) and three wild species(*S. spontaneum* L., $2n$=40-128; *S. robustum* Brandes and Jeswiet ex Grassl, $2n$ = 60 and 80; *S.edule* Hassk., $2n$=60-80) [66]. Some authorities classify the cultivated species of *S.sinense* and *S. barberi* as natural hybrids between *S. officinarum* and *S. spontaneum*. Sugarcane cultivars are interspecific hybrids of up to five parental species. Many cultivars are aneuploids having a large and variable number of chromosomes normally in the range of $2n$ = 110 - 120.

The basic chromosome number in *Saccharum*, as in most Andropogoneae, is generally interpreted as x=10 [67], but the smallest genome size in *Saccharum* is $2n$ = 40 in *S. spontaneum* [68]. In addition, except for *S. officinarum* and *S. robustum*, chromosome numbers do not occur as strict multiples of 10, and opinions vary widely about the size of the basic chromosome number. Parthasarathy [69] and Raghavan [70] suggested that the basic genome was x=5 with 8 and 10 as secondary derivations of this basic number. Darlington and Janaki-Ammal [71] suggested x=10 and 12 as the basic number, while Bremer [72] suggested that there are three basic numbers of x=6, 8, and 10. To the degree that these various suggestions are true, it appears that there has been a parallel evolution of genomes and their polyploid series in the different groups of *Saccharum*. However, since the chromosomes of *Saccharum* are so small (1-3 μm at mid-metaphase) and numerous (40-128), hypotheses about genome structure have been based primarily on distribution of chromosome numbers. Although a RFLP map has been developed in a cultivated sugarcane [73], chromosome maps, needed to resolve questions about the genome structure in *Saccharum*, do not exist.

Recently, quantitative karyotyping of plant somatic chromosomes has been facilitated by computer-aided imaging technology [5] (Chapter 2). Quantitative cytological maps have been made for plants with chromosomes of various sizes and numbers such as barley ($2n$=14) [74], *Crepis capillalis* ($2n$=6) [75] and rice ($2n$=24) [50]. In addition, D'Hont *et al*. [76-78]have effectively applied fluorescence *in situ* hybridization (FISH) methods to examine the basic chromoseome number of the species in the genus *Saccharum* using 45S and 5S ribosomal RNA genes (rDNAs) as probes. Labeled 45S and 5S rDNAs have also been used as probes in multi-color fluorescence *in situ* hybridization (McFISH) to identify homologous chromosomes containing repetitive sequences at the nucleolus organizing regions (NORs) and 5S rDNA loci, simultaneously [24, 79]. This suite of techniques offers the potential for accurately karyotyping the somatic chromosomes of highly polyploid *Saccharum* as the first step in gaining an understanding of the evolution of polyploidy in higher plants.

3.2 Materials and methods

3.2.1 Plant material

The haploid line AP85-361 (2*n*=32), derived from anther culture of clone SES 208 [53], was used in this study. SES 208 is a 2*n*=64 form of *S. spontaneum* that was originally collected in Sevok, West Bengal, India. Both AP85-361 and SES 208 display normal bivalent pairing during meiosis (Chifumi Nagai, HARC, Aiea, Hawaii, personal communication).

3.2.2 Cytology

Fresh root tips were collected, washed, and subjected to a pretreatment in distilled water at 4°C for 12 h. Root tips were then fixed for 1 h in a 1:1 mixture of methanol and acetic acid. Chromosome samples were prepared by the enzymatic maceration/air-drying (EMA) method described by Fukui [48] and Fukui and Iijima [50], with the following minor modifications. The enzymatic maceration was carried out in a 1.5 ml microtube tube at 37°C for 70 min, then the root tips were vacuum-infiltrated for 10 min in the enzymatic mixture before maceration. Chromosome samples were stained with a 2 % Giemsa solution (pH 6.8) for 15 min.

3.2.3 Microscopy and image analyses

Good chromosome samples at prometaphase and mid-metaphase stages were examined and microphotographed using black and white film (Fuji Neopan F, ISO 32, Fujifilm, Tokyo) with the combination developer (Microfine, Fujifilm). Ten good prometaphase chromosome plates without overlapping and with complete chromosome number were analyzed by imaging methods using the condensation pattern (CP) as the key character [50]. Image analyses were conducted by using the four chromosomes of the homologous group as replicates. Seven different prometaphase plates were used in each analysis. The CP and two image parameters, relative length and arm ratio, were measured for all the chromatids, and the data were analyzed statistically. Finally the data from the seven among ten chromosomal plates at the same stage judged from the

total chromosome length were employed to develop a quantitative chromosome map or idiogram. The detailed process of image analysis followed was that described by Chapter 2 and Kato *et al.* [54].

3.2.4 DNA probes

5*S* and 45*S* rDNA probes were prepared by direct PCR amplification from nuclei isolated from root tips of sugarcane using methods previously described for rice [79] and barley [26]. Briefly, root tips were fixed, subjected to enzymatic maceration, and air-dried on a 35 mm, heat-absorptive, film-lined culture dish. Octagonal disks 2 mm in diameter and containing about 100 nuclei were dissected out of the film using an argon ion micro-laser beam through a 100× objective (ACAS 470, Meridian). Each disk with attached nuclei was placed into a 0.5 ml microtube as the source of DNA template. PCR amplification was carried out as described in detail elsewhere [26] using a thermal cycler according to the manufacturer's instructions (Perkin Elmer Cetus). Thirty cycles were used to amplify rDNAs directly from the nuclei. A second run of 30 cycles simultaneously amplified and labeled the PCR products with either biotin-11-dUTP (Enzo Biochemicals) or digoxigenin-11-dUTP (Boehringer Mannheim Biochemica). For the 5*S* rDNA probe, the primer pairs of 21 bases (5'-GATCCCATCAGAACTCCGAAG-3' and 5'-CGGTGCTTTAGTGCTGGTATG-3') were used for amplifying and subsequent labeling in both PCR cycles [79]. In the second PCR cycle, a 70 % substitution of biotin-11-dUTP with dTTP was applied [26]. For the 45*S* rDNA probe, two nested primer pairs were used. The primer pairs (5'-CAATGGATCCTCGTTAAGGG-3' and 5'-TACCTGGTTGATCCTGCCAG-3') were used in the first 30 cycles of PCR [80], and the primer pairs (5'-TAGTCATATGCTTGTCTCAAAGA-3' and 5'-TTGTCACTACCTCCCCGTGT-3') were used in the second 30 cycles of PCR [79]. In the second PCR cycle, 30 % of the dTTP was replaced with digoxigenin-11-dUTP.

3.2.5 Multi-color fluorescence *in situ* hybridization (McFISH)

Chromosome samples exhibiting clear, prominent CP were microphotographed,

and the chromosomes were identified prior to McFISH as described earlier [24, 50]. The samples were destained with 70 % ethanol, and air-dried for *in situ* hybridization. The air-dried slides were treated with 3 μg/ml RNase A (Sigma) in 2 × SSC at 38°C for 60 min. Samples were then completely dehydrated through a 70, 95, and 99 % ethanol series. A 15 μl aliquot of the hybridization mixture containing 100 ng of biotinylated 5*S* rDNA and digoxigenin-labeled 45*S* rDNA in 50 % formamide/2 × SSC was dropped on each slide. The solution was covered with a cover slip, sealed with liquid Arabian gum, and air-dried for 30-60 min. The slides with sealed cover slips were placed on the thermal cycler, that had been modified by addition of an 80 mm × 120 mm cast aluminum, flat plate on the top (Techne, Cambridge, UK). The programmed heating sequence was 70°C for 6 min followed by 38°C for 18 h. The cover slips were removed and slides were washed twice with 2 × SSC, once with 50 % formamide/2 × SSC, and once with 4 × SSC at 38°C for 10 min each. The hybridized probe DNAs were detected by using 20 μl/ml anti-digoxigenin-rhodamine (Boehringer) and 20 μl/ml avidin-FITC (fluorescein isothiocyanate) conjugate (Boehringer). FITC signals were enhanced by a second immunological reaction using 1 % biotinylated anti-avidin (Vector Lab, USA) and 1 % fluorescein-avidin (Vector Lab, USA). Chromosomes were counterstained with 1μg/ml DAPI (4',6-diamidino-2-phenylindole), pH 6.8. Reddish fluorescent signals of rhodamine, greenish fluorescent signals of FITC, and bluish fluorescent chromosomes of DAPI were observed independently by fluorescence microscopy using different filter sets (G15, B10, UV01, Axiophot, Zeiss). Images were recorded separately in three independent image frame memories (768 × 512 pixel matrix with 8 bits of gray steps/pixel) through a high sensitive cooled CCD camera (PXL1400, Photometrics, USA). Following image enhancement, the three images were combined into single merged images by using imaging software (Adobe PhotoShop).

3.3 Results

3.3.1 Polyploidy of the *S. Spontaneum* SES 208 genome

Somatic chromosomes of the anther culture-derived *S. spontaneum* clone at the mitotic mid-metaphase stage are evenly condensed to form short rod shapes, making identification of the individual chromosomes difficult. However, chromosomes at the prometaphase stage are relatively long, showing marked, uneven condensation along the chromosome (Figure 3-1a). The chromosome number of the clone was confirmed as 32, half the number of the anther donor clone, SES 208 ($2n$=64).

Among the 32 chromosomes, four were identified as satellite chromosomes (homologous group 3 of Figure 3-1c). Simultaneous FISH using 45*S* and 5*S* rDNAs revealed four signals of 45*S* rDNAs located at the secondary constrictions on each of these satellite chromosomes (sometimes observed at one side of the satellites) and four signals of 5*S* rDNAs located at the interstitial region on each of four different chromosomes showing identical morphology (Figure 3-1b). These results strongly suggest that this clone is a tetraploid. Based on the condensation pattern (CP) along the chromosomes as the main feature, with chromosome total length and arm ratios as supplementary parameters, the 32 chromosomes were categorized visually into eight groups, of four chromosomes each, displaying similar morphology (Figure 3-1c).

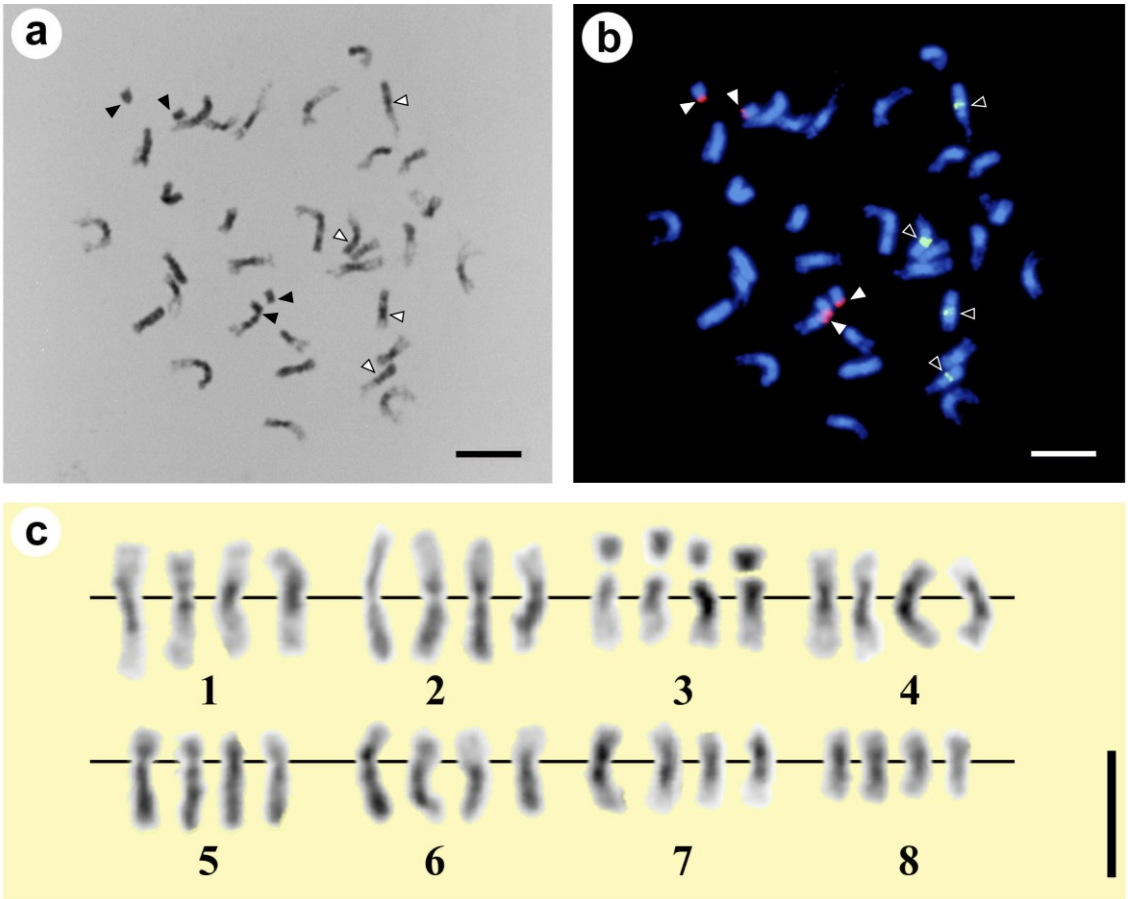

Figure 3-1. Bright-field and fluorescence microscopy of somatic prometaphase chromosomes of the polyhaploid *Saccharum spontaneum* clone AP85-361.

a. Photograph of Giemsa-stained 32 chromosomes showing clear condensation pattern used tentatively to form homologous groups shown in c. Lines show the position of centromere.

b. Multi-color fluorescence image of somatic chromosomes *in situ* hybridized to 45*S* (red fluorescence) and 5*S* rDNA (green fluorescence) probes. Chromosomes counterstained with DAPI. Three of four satellites locate apart from their harboring chromosomes (chromosome3). c. The 32 somatic chromosomes of a single cell of AP85-361 grouped into eight sets of apparently homologous chromosomes. Bars show 5 μm.

3.3.2 Digital karyotyping of *S. spontaneum* chromosomes by image analysis

For each cell analyzed, the image analysis was run in duplicate on each of the four chromosomes of the "homologous" group. Measured values were averaged to give a mean value for each of the eight basic chromosomes of that cell. Results presented are the grand means from 7 different prometaphase plates (Table 3-1). Chromosomes were assigned numbers, ascending from the longest to the shortest in total length, and their images analyzed. An example of the types of the chromosome images gathered for each of the eight base chromosomes of a single cell is displayed in Figure 3-2. For each chromosome, the top panel is the original gray image for the chromosome after staining with a Giemsa solution. The middle panel is a pseudo-colored representation of the original gray image of the same chromosome. The bottom panel is a three-dimensional representation of the original gray image generated by the imaging methods. The right-hand condensation pattern or density profile is an averaged one based on 56 CPs from 7 chromosomal spreads. The averaged CP was defined as standard CP (stCP).

Measurements of arm lengths and the CPs from 7 different prometaphase plates confirmed these cells to be at the same stage of mitosis by a statistical check (α=0.01) of the total length of all chromosomes within a cell. The stCPs of these 7 cells were used to produce a quantitative chromosome map or idiogram of each of the *S. spontaneum* chromosomes (Figure 3-3). The idiogram was produced by first choosing two density values to distinguish three levels of condensation within each chromosome. The upper or lighter density value (gray value=125) approximates the visual boundary between a condensed and a dispersed region of the chromosomes (Figure 3-2). This value also corresponds in the pseudo three-dimensional image to the boundary between a flat and elevated or thick area (Figure 3-2). The lower or darker density threshold (gray value=86) allowed for distinct characterization of each *S. spontaneum* chromosome such as the tertiary constrictions that are observed in chromosomes 2, 5, and 6 (Figure 3-3). The lower density threshold revealed three dense regions unique to chromosomes 2 and 3, two dense regions unique to the long arms of chromosomes 5 and 6, and one dense region in each arm of chromosome 7. Moreover, the lack of a dense region in the largest chromosome 1, the smallest chromosome 8, or the

middle-size chromosome 4 allows these to be clearly distinguishable from the five other chromosomes.

Table 3-1. Mean length (μm) of somatic chromosomes of *S. spontaneum* (clone SES 208)

Chromosome Number	Long arm (mean ±95% CL)	Short arm (mean ±95% CL)	Total (mean ±95% CL)
1	1.957±0.005	1.957±0.005	3.914±0.002
2	1.961±0.006	1.813±0.012	3.774±0.002
3 (without satellite)	1.453±0.004	0.797±0.004	2.240±0.004
3 (with satellite)		1.199±0.004	
4	1.882±0.011	1.314±0.004	3.196±0.002
5	1.920±0.004	1.147±0.004	3.068±0.002
6	1.693±0.004	1.302±0.001	2.995±0.002
7	1.429±0.002	1.400±0.004	2.829±0.002
8	1.213±0.002	1.199±0.004	2.413±0.002

CL, confidence limit.

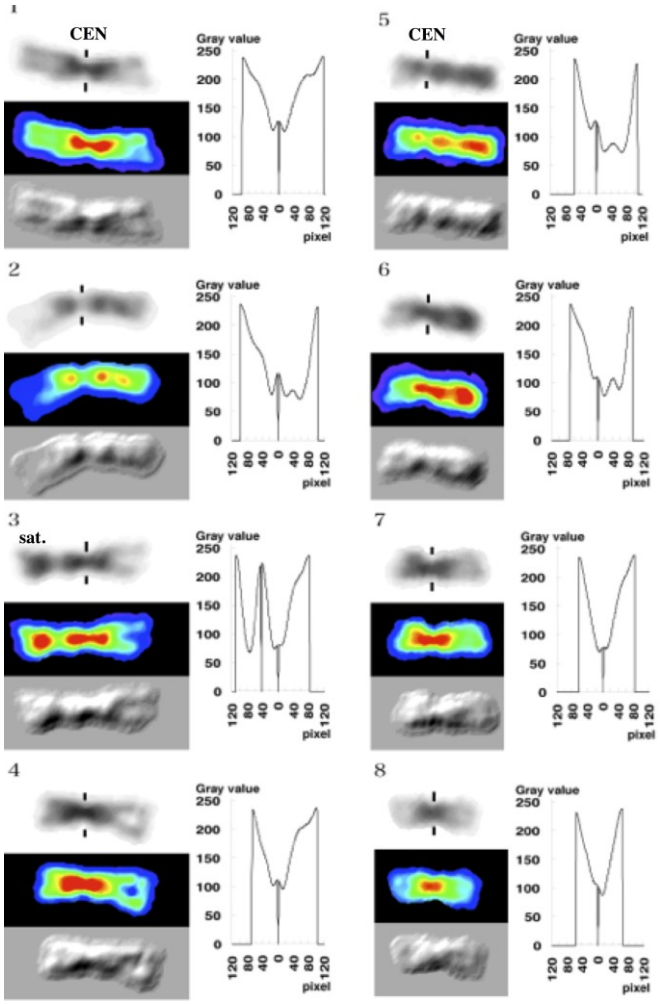

Figure 3-2. One original light microscopic image, two digitally enhanced images, and the average quantitative density profile or standard CP (stCP) of each of the eight basic chromosomes of *S. spontaneum* clone.

For each chromosome the top panel is the original gray image after staining with Giemsa solution. The middle panel is a pseudo-colored representation of the gray image. The bottom panel is a three-dimensional representation of the gray image. The digitally enhanced images gave dramatic improvement of visual recognition of chromosomal fine structures by the different ways. The stCP for each chromosome was calculated by the imaging method described by Kato *et al*. (1997). The stCP satisfactorily represents the original condensation pattern and serves as basic information for development of a quantitative idiogram by setting thresholds of the stCP at the two gray levels.

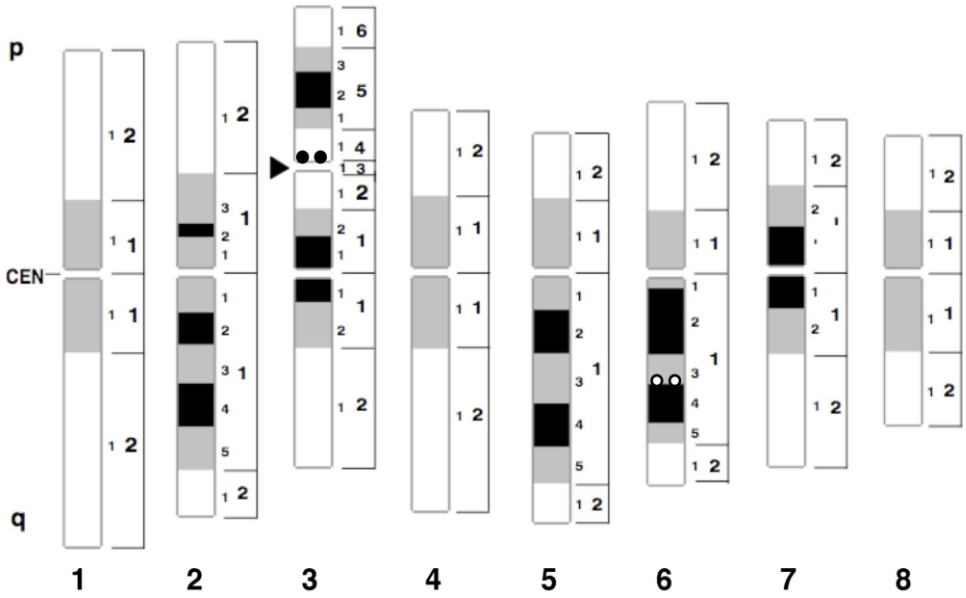

Figure 3-3. Quantitative idiogram of *S. spontaneum* chromosomes constructed on the basis of image analysis data and aligned by centromeric position.

The three densities represent the degree of condensation observed and visually serve as areal landmarks of the chromosomes. The 45*S* rDNA and 5*S* rDNA loci were physically mapped at the specific chromosomal regions of 3p3.1 (solid doublet circles) and 6q1.3 (open doublet circles), respectively.

3.3.3 Mapping 45S and 5S rDNA loci on the quantitative chromosome map

Based on the CPs, the eight basic chromosome groups of *S. spontaneum* can be further subdivided into three groups: (1) chromosomes condensed only around centromere regions (chromosomes 1, 4, 7, and 8); (2) chromosomes with one heavily condensed long arm (chromosomes 2, 5, and 6); and (3) NOR chromosomes (chromosome 3).

The 45*S* and 5*S* rDNA loci were physically mapped to chromosomes 3 and 6, respectively. The locus of 45*S* rDNA was mapped to 3p3.1 of the number 3 satellite chromosome, although signals were sometimes observed at the 3p4.1 region close to the short arm of the separate satellite (Figure 3-1b). The locus of 5*S* rDNA was mapped to 6q1.3 of the number 6 chromosome (Figure 3-3). All results are consistent in indicating that this *Saccharum* clone is a polyhaploid with the basic number x=8.

3.4 Discussion

3.4.1 Basic genome structure of the polyploid *S. spontaneum*

Genetic maps have been developed in many cultivated plants as tools both for molecular and conventional genetic studies. However, until the recent development of molecular marker mapping, genetic maps did not exist for polyploids such as sugarcane, with an exceptional case such as wheat. During this past decade, molecular markers, such as restriction fragment length polymorphism (RFLP), randomly amplified polymorphic DNA (RAPD), and amplified restriction fragment polymorphism (AFLP) have rapidly supplemented traditional genetic mapping in haploid and diploid plants. Generally, however, molecular marker mapping has proven difficult and inefficient for polyploids. This barrier was reduced in *Saccharum* by the production of haploid *S. spontaneum* [53, 81]. Haploid lines were combined with a strategy for identifying single-copy DNA fragments [82], to produce RFLP [83], RAPD [84], and combined RFLP and RAPD [85] genetic maps for *S. spontaneum*. Molecular probes mapping to multiple single-dose restriction fragments allowed the identification of homologous linkage groups that were coalesced to the putative base chromosome number of eight

for the *S. spontaneum* clone SES 208 [85]. An RFLP map for cultivated sugarcane with ten linkage groups has also been developed [73]. However, this is not proof of the basic genome structure; structural analysis of the genome is needed and has been accomplished by the work reported herein.

Knowledge of the polyploidy in *Saccharum* is important not only as it relates to the evolution in sugarcane, but also as it relates to polyploidy of plants in general. The *Saccharum* complex has been reported to have a very wide range of basic chromosome numbers from x=6, 8, 10, or 12 [66, 86]. *S. spontaneum* is a wild species having a wide range of chromosome numbers from $2n$=40 to $2n$=128 [66]. Within this range, five major cytotypes ($2n$=64, 80, 96, 112, and 128) have been reported. It was suggested that the basic number should be x=8 [68]. On the basis of RFLP analyses, da Silva *et al*. [83] also suggested that SES 208 would be $2n=8x=64$. Evidence presented here is the most conclusive that the anther culture-derived clone AP85-361 is a tetrahaploid, with the basic number x = 8, so that its parent clone SES 208 is an octoploid. Based also on the very small morphological differences among homologues of each given chromosome group (Figure 3-1c, Table 1), it is reasonable to consider this line as an autotetrahaploid, and its parent as an autooctoploid. This is in agreement with data showing that segregation of single-dose markers was all in coupling phase and none in repulsion phase [83]. Furthermore the present result is consistent with the basic number of *S. spontaneum* which was suggested by the results of FISH using rDNAs as probe [78]. D'Hont *et al*. [76, 77] also indicated that the basic chromosome number of *S. officinarum* is 10 using FISH. These results, together with the result currently obtained, clearly indicate the effectiveness of the molecular cytological approach not only in determining the physical locations of single-copy nucleotide sequences [87] but also in elucidating the ploidy level of the complex genomes such as sugarcane.

3.4.2 Condensation pattern as a key character for identifying all the *S. spontaneum* chromosomes

Prior attempts to karyotype members of the genus *Saccharum* [88, 89] failed to produce an idiogram capable of distinguishing individual chromosomes. The key

element of the present research that made complete identification and characterization of individual *S. sontaneum* chromosomes possible was the distinctive CP of prometaphase chromosomes. Contrary to conventional perception, the CP appearing at the mitotic prometaphase stage is stable and has significantly greater diagnostic value than the mid-metaphase stage [50, 51]. The size of sugarcane chromosomes at mid-metaphase stage is only 1 to 3 μm. Chromosomes at this condensed stage, which have been used for cytological analyses, lack sufficient details to be distinguished [48, 88, 89]. Unlike earlier work based on the metaphase chromosomes, my present work on prometaphase chromosomes provides the much higher resolution necessary for resolving differences in morphology among all chromosomes of the basic set.

3.4.3 Implications of the quantitative chromosome map of *S. spontaneum*

The idiogram constructed here is the first quantitative cytological map developed for somatic *Saccharum* chromosomes. Every fractional length of each part of the chromosome was quantitatively determined by two density thresholds. Therefore, the chromosome map depicts not only the most distinctive chromosome features, but also numerical values of fractional length of chromosome arms, fractional area of heterochromatin, distribution of differential condensation regions, and their average density, as shown in the idiogram. This idiogram could serve as valuable basic information for visual identification of individual *S. spontaneum* chromosomes since it so closely represents the patterns of individual chromosomes.

The quantitative chromosome map constructed here has several important attributes: (1) the pattern of the idiogram corresponds to the visual pattern of the actual prometaphase chromosomes; (2) the pattern represents the most frequent chromosomal patterns or covers the longest period of mitotic metaphase stage from the prometaphase stage to mid-metaphase stage; (3) all the data shown in the idiogram have a numerical basis, as image analysis methods were employed throughout the study. The chromosome map based on the CP is therefore considered to be not only useful for cytological research, but also fundamental to genetics, molecular biology, and biotechnology on sugarcane and also all the plant species in Gramineae.

Chapter 4.

Development of a quantitative pachytene chromosome map in *Oryza sativa* by imaging methods

4.1 Introduction

Pachytene chromosomes have higher resolution than somatic chromosomes, due to their elongated structure in meiosis. In pachytene chromosomes, linearly arranged, bead-like, compacted segments named chromomeres are observed. Pachytene chromosome analyses are especially effective in plants with small chromosomes [90]. Development of trisomic series in tomato [91], identification of *Arabidopsis* chromosomes [92], and examination of chromosome aberrations in tomato [93], etc. were all performed using pachytene chromosomes. In rice, this approach was developed early, and several reports on pachytene chromosomes were published [94-96] but the results were somewhat divergent. Cheng *et al*. [97] developed a pachytene karyotype, anchored by centromere-specific and *chromosomal* arm-specific molecular markers.

However, there is no literature report on the quantitative image analyses of the chromomeres. Such an objective analysis method, allowing quantitative image analysis of chromomeres, has long been awaited. Previous development of a comprehensive image analysis system for plant chromosome research (CHIAS; [5, 98]), and its subsequently improved versions, i.e., CHIAS II [55] and CHIAS III (Chapter 2) lead us to develop a new imaging method, aimed at the analysis of the more complicated structure of the pachytene chromosomes.

In this chapter, a new image analyzing method for pachytene chromosomes is described. Three different maps, the pachytene chromosome map, the somatic chromosome map and the linkage map of rice chromosome 9 are compared, and the biological significance is discussed.

4.2 Materials and methods

4.2.1 Plant materials

A rice cultivar, Nipponbare (*Oryza sativa* L.) was used throughout the experiment. Anthers, about 0.72 - 0.75 mm in length, were taken from the young panicles and fixed with a fixative (ethanol 3: acetic acid 1). The root tips were excised, treated with the fixative solution and stored at -20°C until use. For longer storage, the

fixative was substituted with 70% ethanol.

4.2.2 Chromosome preparation

After rinsing the fixed anthers in distilled water for about 20 min, pollen mother cells were removed from the anthers, placed on a glass slide and squashed. The slides were frozen on dry-ice, their coverslips removed, and samples were air-dried [99]. Chromosome samples from root tips were prepared according to the enzymatic maceration and air-drying (EMA) method [48, 50]. RNase A treatment (100 μg/ml, 60 min) was performed prior to staining. After 5 min washing with 2xSSC, the slides were dehydrated through an ethanol series (70%, 95% and 99.5%). After air-drying, the samples were stained with a solution containing 1 μg/ml propidium iodide (PI) and 1 μg/ml 4',6-diamidino-2-phenylindole (DAPI). Images of pachytene and somatic prometaphase chromosomes were visualized by fluorescent microscopy (BY60, Olympus) and digitally captured with a CCD camera (PXL1400, Princeton Instrument, USA). Digital images were stored as 12 bit-gray scale images.

4.2.3 Fluorescence *in situ* hybridization (FISH)

The FISH method used was based on a procedure described by Ohmido and Fukui [24] and Ohmido *et al*. [87]. The DNA probe, containing a 3.8 kb insert of 17S-5.8S-25S rDNA (45S rDNA [100]), was biotin-labeled by nick translation. The hybridized DNA was detected with avidin-FITC (Vector Laboratories, USA), followed by biotinylated anti-avidin D (Vector Laboratories) and avidin-FITC (secondary signal amplification).

4.2.4 Image analysis

Digital capture of chromosome images was performed using specialized software (IP Lab Spectrum ver. 3.1.1, Scanalytics Inc., USA) and Photoshop (ver. 3, Adobe Systems Inc., USA). CHIAS III (Chapter 2) was used for chromosome image analysis, after converting the 12 bit gray-scale images into 8 bit images. To measure the length and the fluorescence profile (FP) of the chromosomes, the improved CHIAS III

step1 macro-program [54] was used in conjunction with "Object-Image" (ver.2.06). Object-Image is an extended version of "NIH Image" for Mac OS. The Windows PC version of Object-Image is currently available at ARDI http://www.ardi.com/. CHIAS III software is freely available via the Internet, at: http://www2.kobe-u.ac.jp/~ohmido/cl/chiasIII/index.htm. The "Object-Image" developed at the Institute for Molecular Cell Biology, BioCentrum Amsterdam, University of Amsterdam, is available at http://simon.bio.uva.nl/object-image.html. Chromomere length and FPs were averaged using a step2 macro-program in EXCEL (ver.8, Microsoft, USA).

A calibration curve was calculated for the gray value of each pixel, using the averaged profile lines at the mid-rib of chromosome 9, in both the PI and DAPI images. The satellite region, where the fluorescent patterns of PI and DAPI are quite different, was excluded from the calculation. The gray values of DAPI staining were adjusted to the values of PI, based on the secondary regression equations obtained. The quantitative pachytene chromosome map, or the pachytene idiogram, was drawn using Object-Image and Photoshop.

4.3 Results

4.3.1 Identification of rice pachytene chromosome 9

Chromomeres along the pachytene chromosome were observed with both PI and DAPI staining (Figure 4-1). I confirmed that the PI and DAPI staining showed almost identical patterns along the chromosomes. However, a region of strong PI staining (arrow, Figure 4-1b) and weak DAPI staining (arrow, Figure 4-1c) was also observed at the end of one chromosome within the complement (arrow, Figure 4-1a). At the pachytene stage, a certain chromosomal region was often attached to the nucleolus (Figures 4-1a, f). A nucleolus, shaped as a twin ball or ball (Figure 4-1d arrows, Figure 4-1g), was observed on most nuclear plates as already reported [95]. Thus, most likely, this region was the NOR of chromosome 9, because Japonica rice has one NOR on chromosome 9 in the complement. In addition, partial separation of the homologous

chromosome 9s at the pachytene stage was often observed (arrows, Figure 4-1f). Fluorescent signals (green color) were detected after hybridization with the FITC-labeled 45S rDNA probe (Figure 4-1h), further confirming that this chromosome region was the NOR. Double staining of somatic prometaphase chromosomes revealed two chromosomes with long, stretched, intense PI staining regions (arrows, Figure 4-1e). Two chromosomes, identified as chromosome 9 by their mitotic condensation pattern [50, 101, 102], had the NOR at the end of the short arm.

Figure 11 shows the average fluorescence profiles (FP) along the mid-rib of pachytene chromosome 9 after PI and DAPI staining. The FPs of PI (FP_{PI}) and DAPI (FP_{DAPI}) staining were similar along whole chromosomes, except for the NOR. The highest value in the FP_{PI} was measured at the NOR. The FP_{DAPI}, however, did not show the similar tendency in the same region.

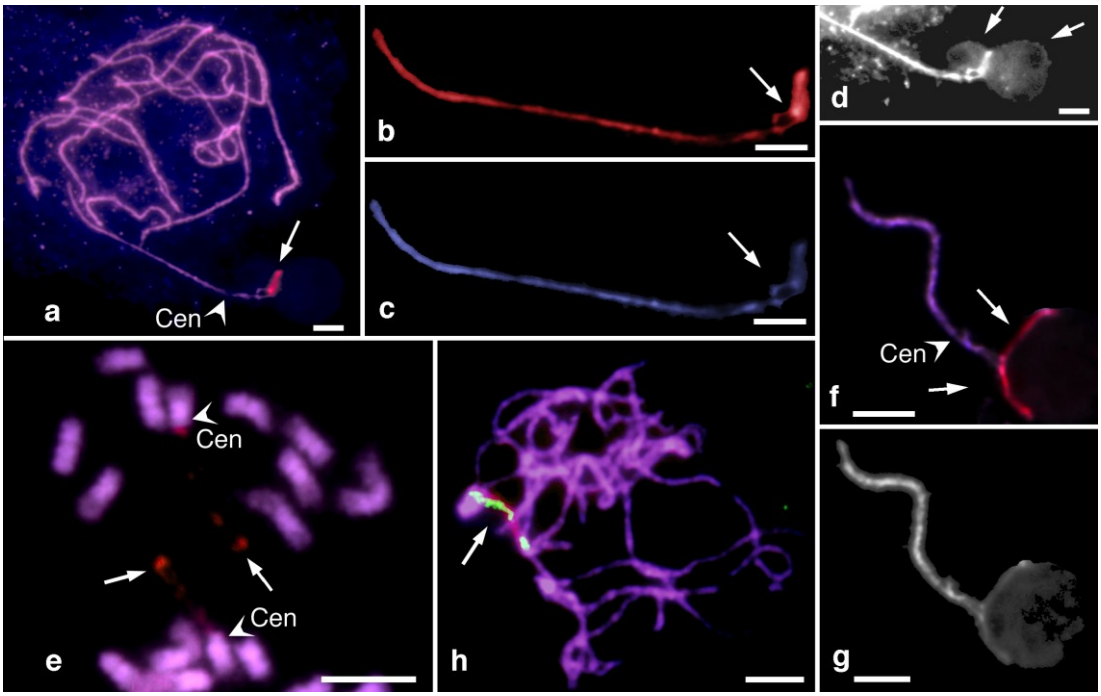

Figure 4-1. Rice chromosome 9 visualized by double staining with PI and DAPI.

a. Pachytene chromosome complement with double staining. Arrow indicates the NOR (nucleolar organizing region) where DAPI stained weakly and PI strongly. "Cen" indicates the centromeric region. b. Rice pachytene chromosome 9 with PI staining. c. Rice pachytene chromosome 9 with DAPI staining. d. A twin-ball shaped nucleolus e. Somatic prometaphase chromosomes. Arrows point to the satellites. "Cen" indicates the centromeric region of chromosome 9. f. Chromosome 9 at mid-pachytene stage. Homologous chromosomes were separated as indicated by arrows, along the NOR. g. A ball-shaped nucleolus. h. FISH on pachytene chromosomes using 45S rDNA as probe. Arrow shows the FISH signals (green) on the NOR. Bars show 5 μm.

4.3.2 Characteristics of chromosome 9

The ratio of the difference in fluorescent intensity between FP_{PI} and FP_{DAPI} at the NOR was 5.75, much higher than in other chromosomal regions (0.80 - 1.28). The fluorescent intensities of DAPI were adjusted to PI for individual chromomeres. I used ten FP_{PI}s from five chromosomes 9, with little overlapping, and statistically at the same stage in the cell cycle, based on their length (26.27 μm - 30.13 μm, 99% confidence intervals) determined by image analysis. The mean length value of the five chromosomes was 27.87 μm (418 pixels). Twenty-two chromomeres were visually identified on chromosome 9. The FP_{PI} was used to develop a pachytene chromosome map, because the FP_{PI} and FP_{DAPI} were similar to each other, and because PI stains DNA regardless of its GC content (Figure 11). The average length of each chromomere was 1.27 μm (19.02 pixels) (Table 4-1). Differences in staining intensity and in length were observed among chromomeres. For example, chromomere No. 14 was short (15.1 pixels) and less condensed. On the other hand, chromomere No. 16 was long (26.0 pixels) with large heterochromatic region.

Table 4-1. Length of each chromomere on chromosome 9.

Meiotic pachytene chromosome						Mitotic prometaphase chromosome
Chromomere (Unit No.)	Length of chromomere (pixels)		Arm symbol	Arm length (μm)	Recombination frequency per μm (CM/μm)	Arm length (μm)
	mean	S.E.				
1	25.0	3.18	sat	5.69	0.00	-
2	20.6	3.16				
3	16.4	1.07				
4	23.4	2.25				
5	20.7	3.43	p	3.75	0.21	0.52
6	17.5	3.14				
7	18.1	2.79				
8	22.2	2.91	q	18.40	5.18	2.11
9	23.3	2.12	(a)	(7.39)		
10	16.0	1.34				
11	14.9	1.46				
12	19.0	3.39				
13	15.5	1.39				
14	15.1	2.96	q			
15	19.6	1.54	(b)	(11.01)		
16	26.0	1.92				
17	16.2	2.06				
18	18.8	2.16				
19	15.2	1.42				
20	16.2	0.87				
21	18.4	3.45				
22	19.6	1.77				
Average	19.0	2.26			3.45	

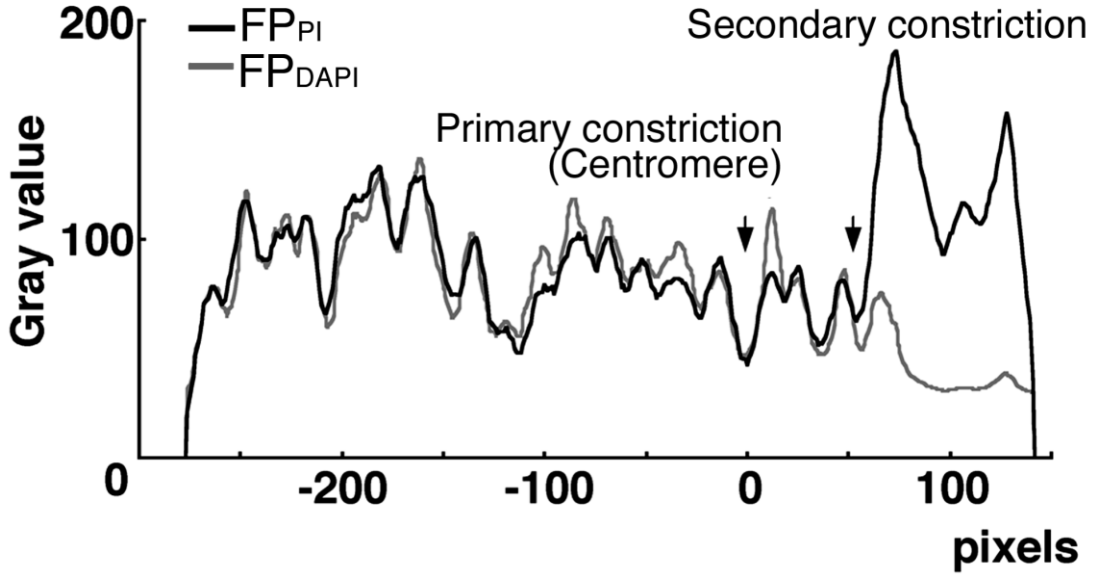

Figure 4-2. Comparison between FP_{PI} and FP_{DAPI} of pachytene chromosome 9 after PI and DAPI staining.

Bold black and gray lines represent the FP_{PI} and FP_{DAPI}, respectively. Arrows show primary and secondary constrictions.

4.3.3 Image analysis of the pachytene chromosome 9

Figure 4-3 depicts the three major steps of the procedure for mapping of a pachytene chromosome.

1st step: Two chromosome images, of PI (Figure 4-3a) and DAPI (Figure 4-3b) staining, were stacked and handled as a single image. After noise reduction and normalization of gray levels, midrib-lines were interactively drawn along pachytene chromosome 9 (Figure 4-3d). Using the PI and DAPI chromosome images as the references, segmented line-shaped ROIs ("regions of interest") were interactively drawn at the boundaries between any two chromomeres in these images, and were laid over the 0-gray-level binary image (white) with 255-gray-level (black). Individual chromomeres were numbered, and each chromomere region was pseudo-colored based on its chromomere number (Index image; Figure 4-3c). The gray values of FP_{PI} and FP_{DAPI} along the midrib-line of each homologous chromosome (Figures 4-3a, b) and the length of each chromomere region of the Index image (Figure 4-3c) were obtained.

2nd step: The average of FP_{PI} values and the length values of each chromomere were measured using the ten FP_{PI} (five chromosomes), and were stored.

3rd step: A bar image of the average chromosome width was developed from the average FP_{PI} values, converting black (gray value = 255) to white (gray value = 0) (Figure 4-3e: FP_{PI} image). The two intermediate images (Figures 4-3g, h) obtained from the FP_{PI} image plus the Chromomere index image (Figure 4-3i) lead to the development of the Index idiogram (Figure 4-3k). Combination of the two intermediate images (Figures 4-3g, h) with the binary bar image (Figure 4-3f) generated a Condensation pattern idiogram (Figure 4-3j). The intermediate images were produced as follows,

1) Local mean gray values of FP_{PI} were subtracted from the gray values of FP_{PI} (Figure 4-3e). Afterwards, dark stained and light stained regions were determined setting the local mean values as standard. Thresholding the dark and the light regions of Figure 4-3e, followed by binarization, which is converting 255-level gray-scale images into black-and-white (darker regions, black and blighter regions, white), yielded a banding pattern (Binary image; Figure 4-3f).

2) A smoothing filter treatment, acting vertically across the midrib-line of the

chromosome was applied to the FPPI image (Figure 4-3e) and a filtered image (Figure 4-3g) was obtained.

3) The contour line of the filtered image was obtained and subjected to binarization (Outline image; Figure 4-3h).

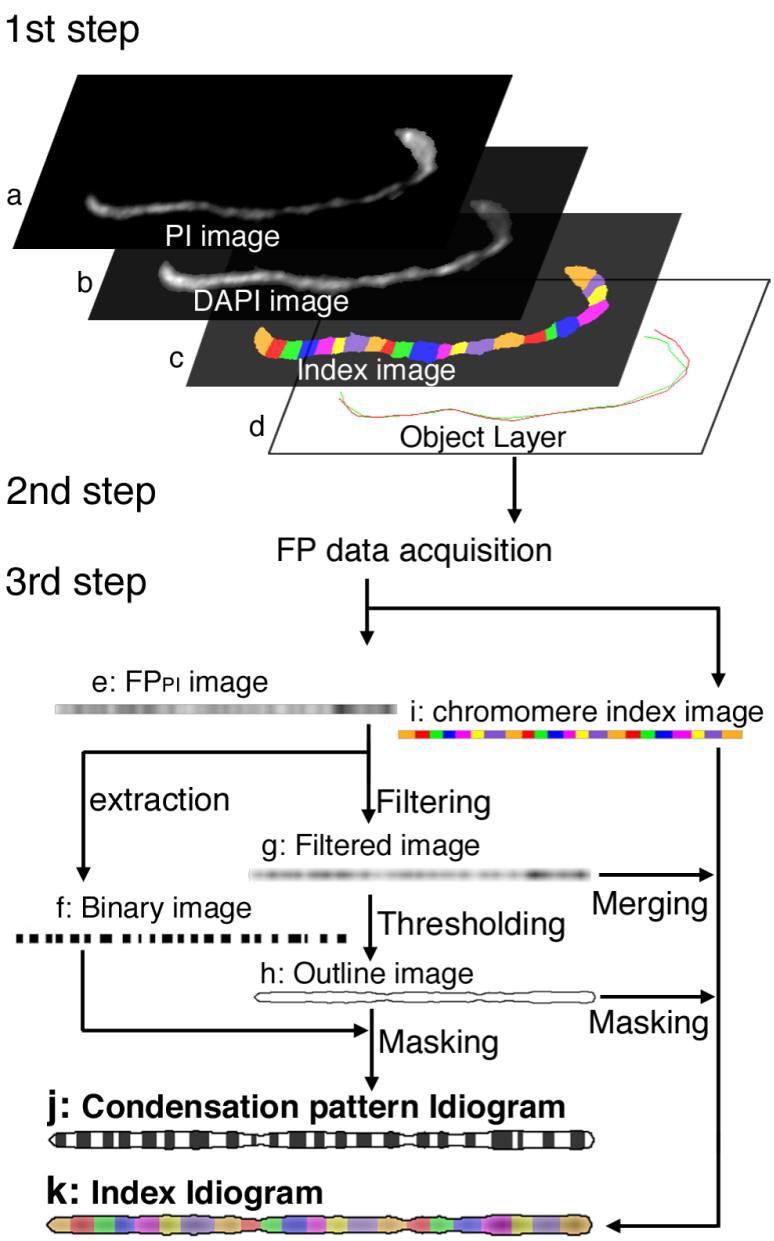

Figure 4-3. Representative steps for development of a pachytene chromosome map.

Starting from two images of chromosome 9 stained with PI and DAPI, two idiograms showing heavily condensed regions within each chromomere (Condensation pattern idiogram) and each chromomere (Index idiogram) were generated through three major steps.

Figure 4-4 details the process by which the condensed and de-condensed regions of the chromomeres are defined. These regions were initially observed as bright or dark regions on the stained chromosome. The bold line in the graph shows the FP_{PI}, whereas the gray line shows the locally averaged values calculated by the moving average. Subtraction of the averaged values from the original FP_{PI} values results in an up-and-down line on the X-axis. Each region above the X-axis of the graph corresponds to a condensed or light region. The subtracted gray values of the pixels were replaced with the averaged median value of three successive pixels in order to remove the small fluctuation of gray values. As a result, I obtained the standardized data for development of an idiogram with the information of condensation patterns and the position of the chromomeres.

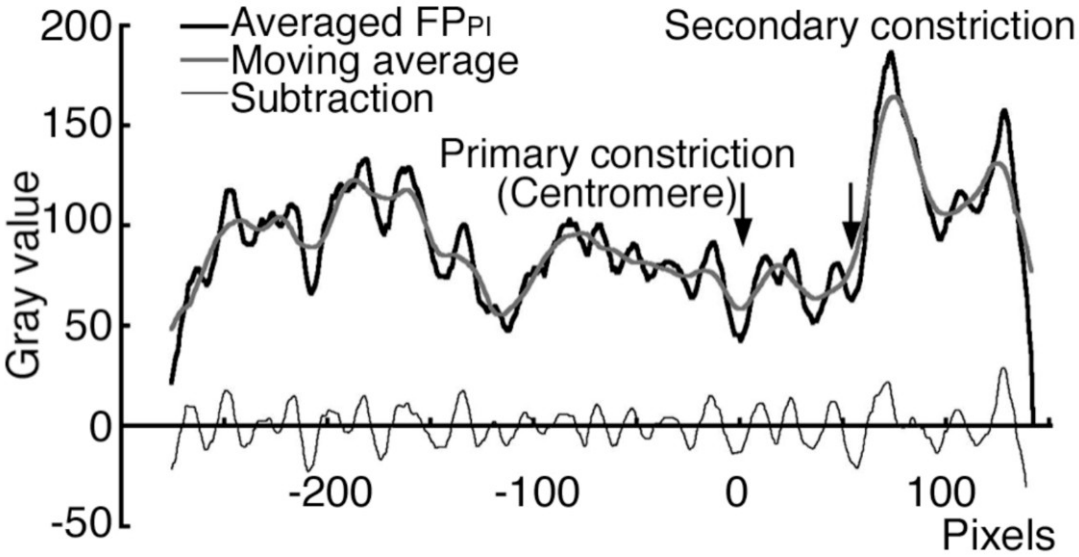

Figure 4-4. Extraction of the condensed regions from chromomeres of chromosome 9.

Subtraction of the moving average from averaged FP_{PI} yields the condensed region within each chromomere along the chromosome.

4.3.4 Comparison of three maps: the pachytene chromosome, the somatic prometaphase chromosome and the linkage map of chromosome 9

Figure 4-5 shows the somatic chromosome map [50, 102] , the pachytene chromosome map currently developed, and the linkage map (RGP Public Data, http://web.staff.or.jp/), adjusted for chromosome length. Eight addresses are mapped on the somatic prometaphase chromosome map, and 48 addresses on the pachytene map, with 22 chromomeres. The arm ratio (satellite region excluded) of the prometaphase chromosome 9 is 3.90 [50] (, whereas that of the pachytene chromosome 9 is 4.92. The arm ratio of the linkage map is 119.13. The overall recombination frequency per unit length (cM/μm) was 3.45 for the pachytene chromosome 9, with values of 0.21 for the short arm and 5.18 for the long arm (Table 4-1). Centromeric positions are more or less similar between the prometaphase and pachytene chromosomes. However, the position of the centromere on the linkage map (RGP Public Data, http://web.staff.or.jp/) was quite different from those of the two maps. NOR positions were also different, even between prometaphase and pachytene chromosome maps. NOR position in the linkage map can be explained either by lack of its recombination or by lack of detection.

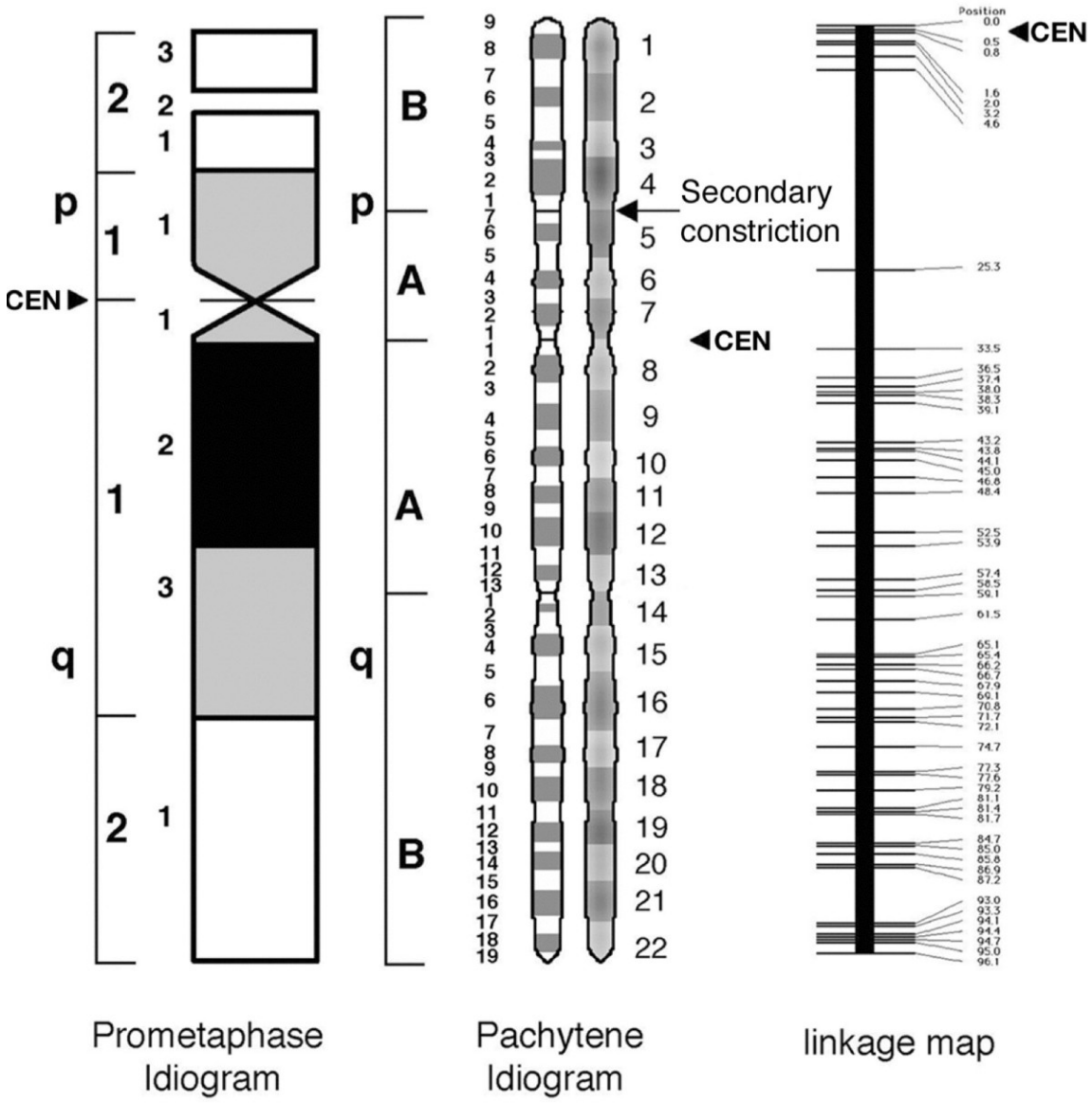

Figure 4-5. Comparison of the three chromosome maps of rice chromosome 9. From left to right, idiogram for somatic prometaphase stage, idiograms for pachytene chromosomes (Condensation pattern idiogram, Index idiogram), and linkage map.

4.4 Discussion

4.4.1 Rice chromosome 9

In this chapter, structural characteristics of rice pachytene chromosome 9 were defined by image analysis. A study of rice pachytene chromosomes was first reported by Shastry *et al*. [94]. Kurata *et al*. [95] and Khush *et al*. [96] also studied rice pachytene chromosomes using Japonica and Indica rice, respectively. In their reports, there was no description of the satellite regions, probably because ordinary staining (such as Giemsa staining of the nucleolus) interfered with the detailed observation of the NOR and the satellite region at the nucleolus. The idiogram currently developed is consistent with that of Kurata *et al*. [95] except for the NOR and satellite region. Three chromomeres located within the NOR and satellite region were newly identified by the present study.

DAPI and PI stained the NOR and satellite region differently, as described in my study. PI is a cationic fluorochrome classified as a phenonthridium-type dye, which intercalates within the double helix structure of deoxyribonucleic acids. DAPI is a specific intercalator for AT base pairs of DNA. Past and present research indicates that the NOR is a GC-rich region. Using a double staining technique with CMA (Chromomycin A3) and DAPI, Lorite *et al*. [103] reported that the NOR had a high GC content. The 45S rDNA, which is the main component of the NOR, shows 60-70% GC content in the coding regions (DNA Data Bank of Japan, http://www.ddbj.nig.ac.jp/). It was also reported that the spacer regions have a GC content of 70.17%, even higher than the coding regions [104].

4.4.2 Image analyses

Computerized image analysis, to characterize the chromomeres of pachytene chromosomes, has not been available in the past, because the size and fluorescence intensity of chromomeres are quite different from each other. In this study, I established

a method to evaluate gray values relative to adjacent regions, to help me discriminate the condensed, chromomeric regions, distributed along the axis of the pachytene chromosomes. The procedure described in this manuscript is based on a method previously developed to extract C-band positive regions in *Crepis* chromosomes, simulating the human visual sense [75]. The main difference from the previous method is that the current one uses a one-dimensional smoothing method, instead of applying a two-dimensional low-pass filter. The reason for this change is that the result of a low-pass filter treatment of the image was significantly influenced by the gray values of the pixels outside of the chromosomal regions, especially in constricted regions such as the centromeres. The current method was proven to be very effective for the outlining of the condensed regions of the chromomeres. Dawe *et al*. [105] and Peterson *et al*. [106] also analyzed pachytene chromosomes, using either three-dimensional imaging methods in maize, or FISH methods in tomato, respectively. My procedure is a alternative approach to pachytene chromosome analysis, which produces quantitative chromosome maps with banding landmarks, similar in aspect to the well-known G-banding of vertebrate chromosomes.

4.4.3 Advantages of pachytene chromosome mapping

There are two major advantages in using the quantitative pachytene chromosome map for genetic research. First, in gene mapping, the pachytene chromosome map is more suitable for detailed allocation of genetic information, because more addresses can be assigned on pachytene chromosomes (1 pixel = 67nm) than on prometaphase chromosomes. This also allows a higher resolution gene mapping by FISH on pachytene compared to somatic chromosomes. Cheng *et al.* [107] developed a physical map of rice pachytene chromosome 10, by FISH mapping of bacterial artificial chromosome (BAC) clones. Combining my imaging system with FISH mapping of DNA markers (e.g., genomic anchor clones, cDNAs and transgenic DNAs) would reveal a more accurate physical position of genes and other DNA probes along rice chromosomes.

Second, mapped chromomeres can easily serve as a landmark for precise

positioning of structurally unique features, such as heterochromatic and euchromatic regions. Morphological characteristics observed and described in the pachytene chromosomes could not be detected in the corresponding somatic chromosomes. For example, the constriction between the chromomere Nos. 13 and 14 was confirmed only in pachytene chromosomes. The same was true for chromomeres Nos. 16, 17 and 18 which cover the heterochromatic region. These minute morphological characteristics may serve as clues for the analysis of higher chromosomal structures.

On a linkage map, the distance between two loci is measured by recombination frequency, with the assumption that the recombination frequency is even throughout the chromosome. However, there are several reports of uneven recombination frequencies along chromosomes [74, 108, 109]. It is likely that, by combining the pachytene chromosome map with the linkage map, better understanding between the recombination frequency and the unit-length of a chromosome can be obtained. This would result in a more accurate, integrated chromosomal map.

I believe that the pachytene chromosome map carries important biological information which is not replaced by the other maps. In combination with other procedures, it could play a crucial role in developing highly integrated chromosomal maps.

Chapter 5.

Image analysis of small plant chromosomes by using an improved system, CHIAS IV

5.1 Introduction

As a part of the genome-analysis projects for legume crops, researchers have constructed high-density genetic linkage maps for these plants and mapped a large number of molecular markers that are useful or even indispensable for studies in various scientific fields, including comparative genomics, gene identification, gene isolation, and marker-assisted breeding [110]. Genetic maps of red clover have recently been developed by using molecular markers [111, 112]. Although conventional N- or C-banding methods are effective for the identification large chromosomes, i.e., chromosomes of faba bean (*Vicia faba* L.), they are not as effective for the identification of small chromosomes with lengths of about 1-3 μm at metaphase, e.g., chromosomes of *Lotus japonicus* (Regel) Larsen, red clover (*Trifolium pratense* L.), and soybean (*Glycine max* L.). Further, although chromosomes can be visualized as a genomic substance under a microscope, quantitative analysis of directly visualized chromosomes is difficult. However, some approaches for such assessments have been reported [5, 55, 113].

Thus, although identification of individual chromosomes is a difficult process, objective evaluation of the morphological characteristics of small plant chromosomes is essential [114]. Fukui and Mukai [98] and Fukui and Iijima [50] used the first-generation chromosome image analyzing system (CHIAS) and observed specific condensation patterns (CPs) in small plant chromosomes at the somatic prometaphase stage. However, the specific software programs used in their study were not available to all researchers. The image analysis methods in the second- and third-generation CHIAS used CPs as a standard parameter for identification of small chromosomes, thereby enabling chromosome identification and quantitative chromosome mapping [115, 116]. An objective image-analysis method can avoid personal subjectivity of judgment and prevent vague descriptions in the development of a chromosome map.

In the present study, I developed the fourth-generation CHIAS (CHIAS IV), which incorporates improved automation in the analysis procedure. To demonstrate the performance of the system, I employed CHIAS IV for the analysis of fluorescence *in situ* hybridization (FISH) mapping data using several markers on the somatic

chromosomes of *T. pratense*. The combination of the quantitative chromosome map and the genome-sequence data will serve as a powerful tool to promote plant-genome and genetic studies.

5.2 Materials and methods

5.2.1 Chromosome images and implementation of the system for image analysis

In this chapter, I used images of the somatic chromosomes of red clover (*T. pratense* L., $2n = 2x = 14$); these images were obtained at the prometaphase stage of mitosis. For the CHIAS analysis, I used images obtained from FISH mapping performed using ribosomal RNA genes (26S rDNA) and bacterial artificial chromosome (BAC) clones in red clover plants supplied by Kazusa DNA Research Institute [112]. The images were converted into red-green-blue(RGB) images with 8 bits per channel by using IPLab Spectrum^{TM} software, Version 2.4 (BD Biosciences Bioimaging Rockville, MD, USA). Nuclear images showed little overlap between the chromosomes and revealed the positions of rDNA and the BAC clones were chosen for the following image analysis procedures.

5.2.2 CHIAS IV

CHIAS IV is an improved version of CHIAS [5, 98] to develop for chromosome identification and facilitate quantitative chromosome mapping. The CHIAS IV upgrade was built on CHIAS II [55] and CHIAS III (Chapter 2). The functionality of CHIAS has been improved by the addition of pseudo-color processing, an automatic process for sorting chromosomes, and a utility to measure the chromosome lengths and arm ratios. All procedures—from the input of the chromosome images to the drawing of the chromosome map—are automated in this version. The CHIAS IV program and an instruction manual can be downloaded from the following site: http://www2.kobe-u.ac.jp/~ohmido/index03.htm

5.2.3 Development environment for CHIAS IV

CHIAS IV is based on the public-domain image-processing software ImageJ, which was developed by the National Institutes of Health (NIH; Bethesda, MD, USA) by using the Java programming language [117]. Java for Mac OSX (version 1.60.17, 32-bit) was used as the development language. The CHIAS IV program source file was compiled using the Java compiler associated with ImageJ.

CHIAS IV runs on personal computers employing Windows XP and Mac OSX operating systems. ImageJ is the host application for CHIAS IV; for both operating systems, the software requires version 1.42 of ImageJ (http://rsb.info.nih.gov/ij/download.html) and Java version 1.4 or later (http://www.java.com/). The CHIAS IV plugin file must then be installed. The "CHIAS4_.jar" file was obtained from http://www2.kobe-u.ac.jp/~ohmido/index03.htm.

5.3 Results

5.3.1 Operation of CHIAS IV for plant chromosome analysis

Processing by CHIAS IV is significantly more automated than that by CHIAS III. The new system was developed to reduce the difficulties associated with the analysis of small chromosomes, such as the chromosomes of *Lotus japonicus* (Miyakogusa), *Oryza sativa* (rice), *Saccharum spontaneum* (sugarcane), and *Brassica* species [61] (Chapter 3). CHIAS IV analysis of the red clover chromosome images obtained at prometaphase comprises the following 3 steps shown in Table 5-1: measurement of the fluorescence profile (Step 1, Figure 5-1, and Figure 16), calculation of the standard fluorescence profile (Step 2, Figure 5-3), and construction of an idiogram or quantitative chromosome map (Step 3, Figure 5-3).

Table 5-1. Operation of CHIAS IV

1. Step 1—Measurement of the condensation pattern (CP) or fluorescence profile (FP)		
	Operation	Explanation of operation
1.1	Open image	An image is opened as an RGB stack.
1.2	Extract chromosomal regions	Chromosomal regions are extracted from the image after regional adjustment of the threshold.
1.3	Separate close and/or overlapping chromosomes	The chromosomes that are close to each other are separated manually.
1.4	Extract signal regions	FISH signal regions of the BAC clones are extracted. If the signal is scattered, this step of the process can be omitted.
1.5	Add ID	Chromosome numbers are automatically added to all chromosomes by area order.
1.6	Sort (and normalize)	Chromosomes are sorted in a region of interest (ROI) according to their name order. Then, the chromosomal orientations are corrected for a vertical alignment. The image is enlarged by a factor of 2 to prevent image-quality deterioration during the rotation process. Simultaneously, the range of the gray level of the chromosome region is normalized to 1-255.
1.7	Rotate chromosome	The top (short arm) and bottom (long arm) of the chromosome are turned upside down.
1.8	Detect centromere	The chromosomal arms are separated at the centromeric region.
1.9	Index labeling	An index-label layer is added to the 3 RGB layers. Labels are inserted for segments of the chromosome regions. This operation should be executed only when regional segmentation is necessary.
1.10	The measurement of CP or FP	A line is drawn along the midrib of the chromatid, and the CP or the FP on the line is measured.
Step 2—Create a standard profile		
2.1	Average the profile (“AVG” tool)	The profile data of homologous chromosomes are averaged.
2.2	Align all colorgrams of the chromosomes (“Align” tool)	All measured chromosome colorgrams are aligned to one image by using their centromere regions.
Step 3—Create an idiogram		
3.1	Create graygram	The averaged graygram of the counterstain layer obtained in Step 2 is created by using the Otsu method for automatic thresholding.
3.2	Fix condensed regions	The first threshold in the gray level is determined. The gray areas (i.e., condensed regions within a chromosome) of the chromosomes are identified.
3.3	Fix highly condensed region	The most condensed area is determined. The black areas of the chromosomes are identified.

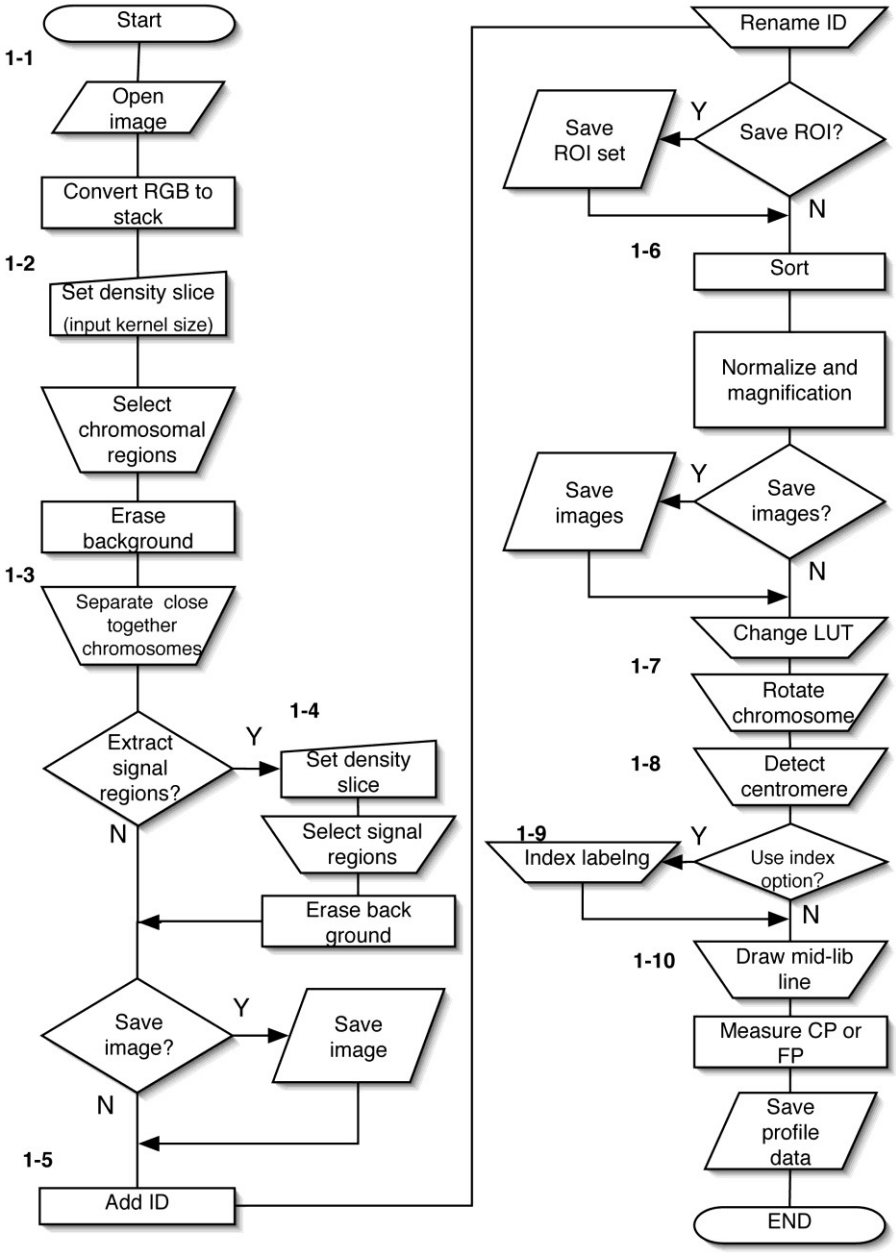

Figure 5-1. A decision flowchart detailing Step 1 of the CHIAS IV procedure.

In this study, CHIAS III could use 24-bit images only if the images were in a 3-slice 8-bit (RGB) stack format; however, CHIAS IV afforded better image visibility, thereby allowing direct processing of 24-bit color images. Extraction of chromosome region, addition of chromosomal ID, sorting of chromosomes, detection of the centromere position, and measurement of CP or fluorescence profile (FP) were performed during the first step. The process for extraction of the chromosomal region is similar to that used in CHIAS III, but the automatic chromosomal ID processing by area order is a new feature in CHIAS IV. Chromosomes were automatically sorted by renaming these IDs.

The measurement of the FP of each grayscale slice of the RGB image was performed concurrently. Fluorescence intensities of counterstaining (4',6-diamidino-2-phenylindole, DAPI: blue, B image) and multicolor signals (cyanine 3, Cy3: red, R image and fluorescein isothiocyanate, FITC; green, G image) were measured, and the profile image of each chromatid was developed automatically (protocol 1.10, "CP" command). This profile image called a "colorgram" represented each FP of the RGB image.

The second step in the new CHIAS IV protocol is significantly different from that in CHIAS III. In this step, the data in a colorgram bar is saved in the TIFF format (Figure 5-3c), and the operations that were performed in Microsoft Excel in CHIAS III are performed within ImageJ itself in CHIAS IV. In addition, each channel of RGB and the index label can be processed simultaneously. At the beginning of the second step, the averaged colorgram profile data from each chromatid of homologous chromosomes were measured (protocol 2.1, "AVG" command). Averaged colorgrams were displayed on the basis of the centromere (protocol 2.2, "Align" command).

In Step 3, condensation regions (protocol 3.1, “Thres,” “FixG,” and “FixB” commands) were identified, and the construction of the idiogram or quantitative chromosome map was completed (Figure 5-3d). Condensed regions, noncondensed regions, and intermediate regions were displayed as black, white, and gray images, respectively. Condensed regions were determined by a 2-step thresholding procedure. CHIAS IV employed the Otsu method [118] for automatic thresholding (Figure 5-3d), which is different from the method used in CHIAS III. The Otsu method is based on discrimination, and least-squares criteria are used for standard binarization. The idiogram was then created using the counterstain layer. Comparison of the FISH signals was easy, because the FISH signals were conserved in another layer of the colorgram.

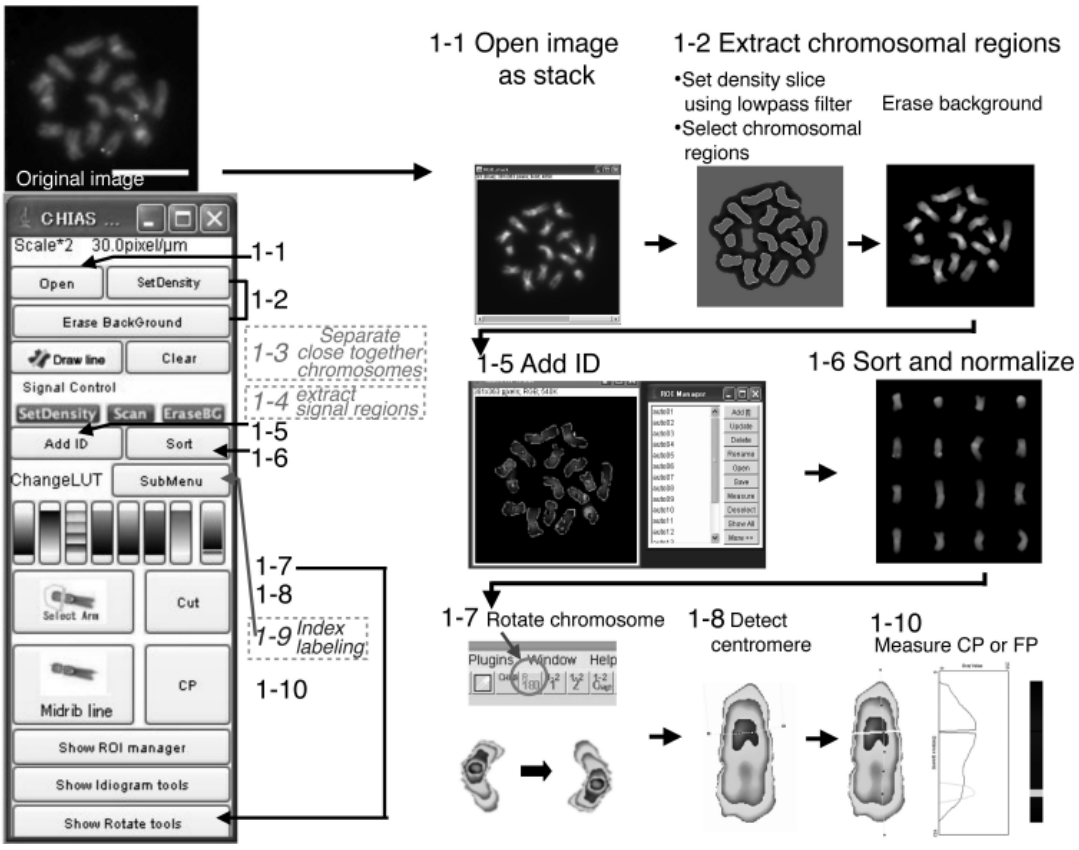

Figure 5-2. Analysis by CHIAS IV, Step 1

The window displayed at the left edge is a CHIAS menu window. The process descriptions for protocols *1-3, 1-4*, and *1-9* are added for convenience.

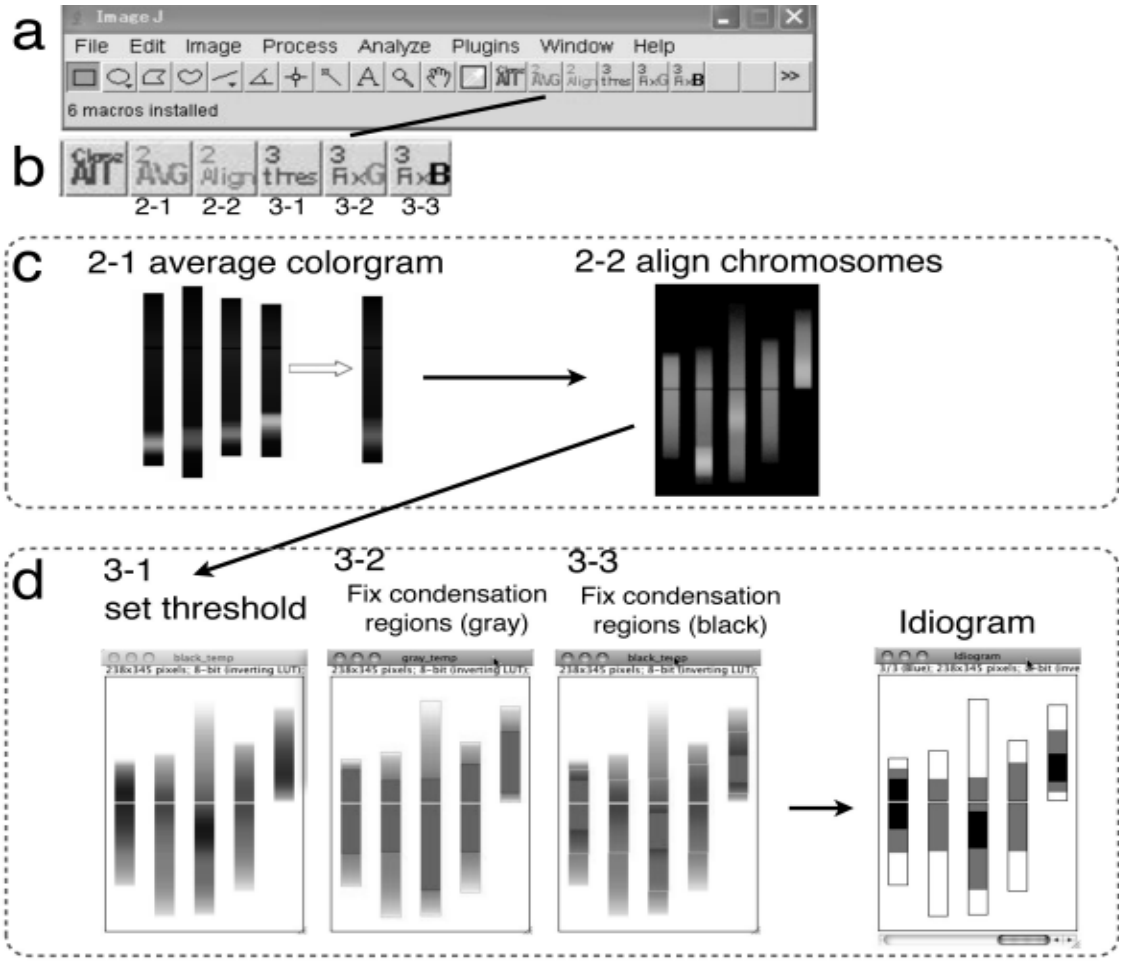

Figure 5-3. Analysis by CHIAS IV, Steps 2 and 3.

(a) An ImageJ menu. Idiogram tools are displayed on the ImageJ toolbar in the menu. (b) An enlarged picture of the tool bar. (c) The protocol of the second step. (d) The protocol of the third step.

5.3.2 Combined efficacy of CHIAS IV and FISH in the analysis of somatic prometaphase chromosomes of red clover

Figure 5-4 shows the chromosomes sorted according to the area order by using the automatic sort function. Chromosomes 1, 3, 6, and 7 were identified by the positions of the FISH signals for the ribosomal RNA gene. Several homologous chromosomes were disassociated by the sorting order of the chromosomal areas. This disassociation can be remedied by adding the information from the FISH signals to the ID. Figure 5-4e shows the chromosomes sorted according to the chromosome numerical order determined from FISH signals after directional adjustment of the chromosome arms. The rest of the chromosomes with no FISH signals were arranged according to the area order (Figure 5-4f).

In CHIAS IV, measurements are performed using the index label. The index-label function of CHIAS III was developed to perform identification using pachytene chromosomes (Chapter 4). Figure 5-5 shows the CP profile and a colorgram bar. The advantage of the colorgram bar is to afford easy visual interpretation of chromosome characteristics. In addition, the text data of each RGB profile is easily obtained from the colorgram bar by measurement of the profile in ImageJ. Further, the peak regions of the FISH signals and the ranges can be easily filled in by labeling the data with a pseudocolor palette. During pseudocolor labeling, an index label is displayed along the right edge of the colorgram bar.

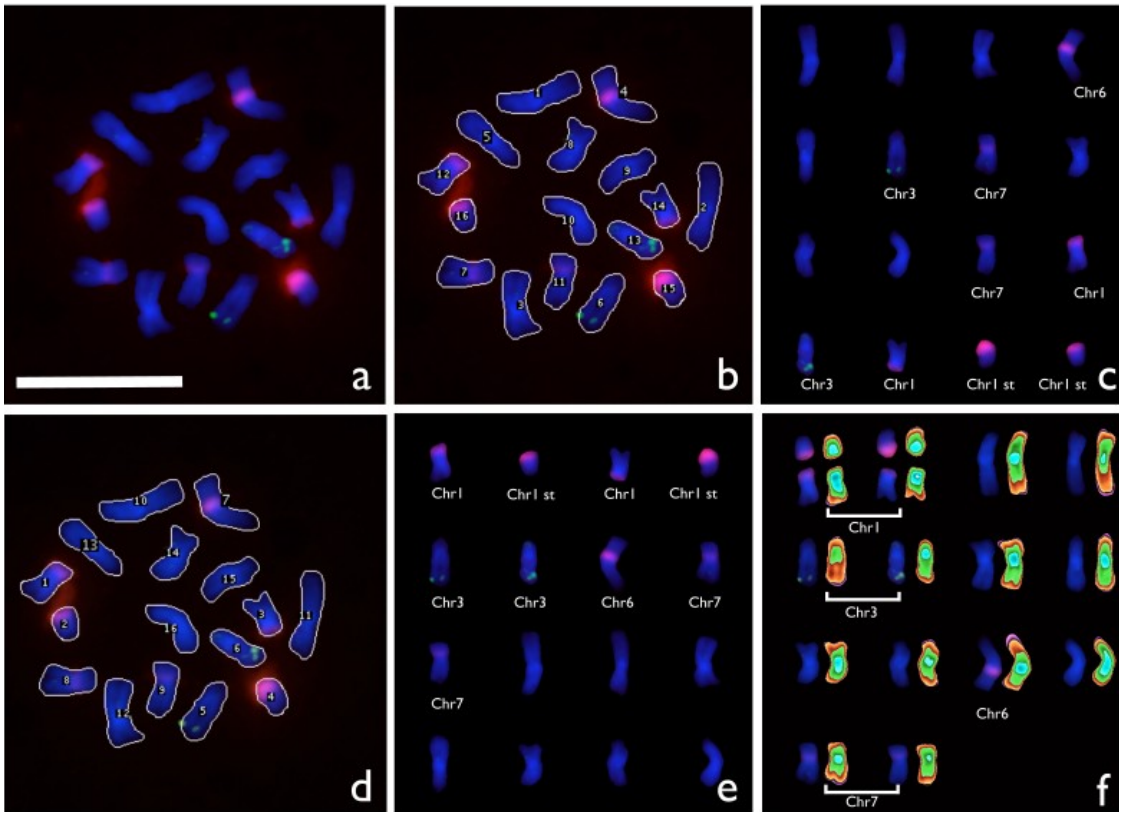

Figure 5-4. The sort function in CHIAS IV.

(a) The FISH image obtained using rDNA (red) and a BAC clone (green) as probes. The red signal represents 26S rDNA, and the green signal represents a BAC clone on chromosome 3. The bar indicates 10 μm. (b) Addition of the ID by the automatic sorting function. (c) An automatic sort image. (d) Adjustment of the ID on the basis of the signal information. (e) Sorting based on signal information. The chromosomes without signals are displayed according to their area order. (f) The image sorted in chromosome numerical order. The right-side images are the ones obtained after pseudocolor processing.

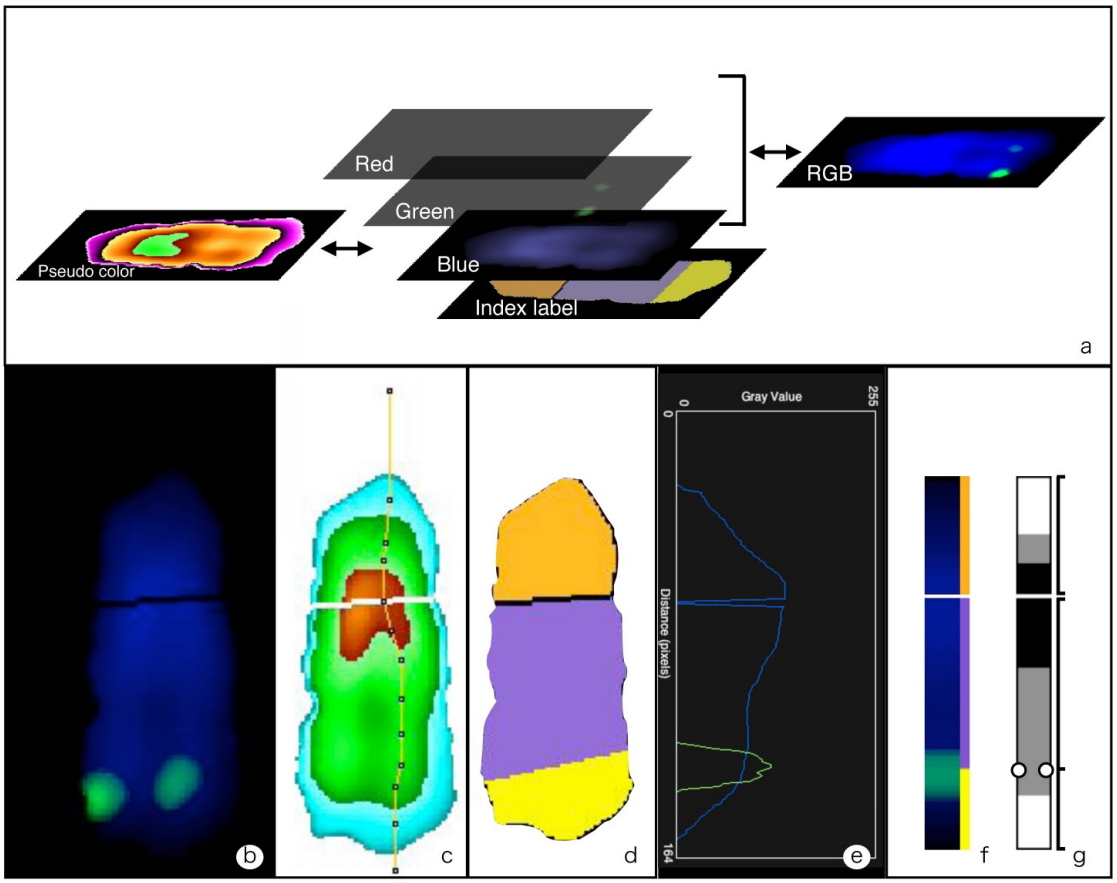

Figure 5-5. The segmentation of chromosome regions by using index labeling.

(a) Constitution of the color image and the index labeling. The visibility of counterstain (blue) slice density was improved by a pseudocolor display. This image was converted into three 8-bit grayscale images by changing a 24-bit RGB color image into a stack image. (b) In the RGB color image of chromosome 3, the green spot shows the signal of a BAC FISH probe. (c) Pseudocolored image from counterstained slice. (d) The index-label image. Orange (gray value 1), cyan (gray value 2), and yellow (gray value 3) are shown by pseudocolorization. (e) The FP from the midrib line of the chromosome. (f) A colorgram image created from the FP measurement. The index label is arranged next to the colorgram bar, and the pseudocolor is displayed, but it con- sists of gray values. (g) Idiogram development from a colorgram.

5.4 Discussion

5.4.1 Significance of chromosome image analysis by CHIAS IV

Objective identification of chromosomes and quantitative chromosome mapping form the basis for the analysis of plant chromosomes [119, 120]. Chromosome maps of barley [74], *Crepis* [75], and *Saccharum officinarum* (Chapter 3) were developed using CHIAS, CHIAS II, and CHIAS III, respectively. Image analysis has been determined to be effective in objective identification of the small-sized chromosomes of *O. sativa* [50, 102] and *Arabidopsis* [115].

Recently, somatic prometaphase and pachytene chromosomes of the model legume plant, *Lotus japonicus,* were analyzed using CHIAS III [116, 121], and the process was further validated in red clover chromosomes. In this study, I have demonstrated the effectiveness of image analysis in the allogamous legume, red clover, by using CHIAS IV. In comparison with CHIAS III, CHIAS IV affords improved automation in the analysis procedure and ensures that the manual operations in Microsoft Excel are unnecessary for the standardization of CPs. Another improvement in CHIAS IV is that the program automatically sorts chromosomes. As a result, the analysis time for each chromosome spread was dramatically shortened to about one-third of the time required for analysis using CHIAS III. Currently, manual analysis of one chromosome plate requires about 30 min. Further, measurement by manual operation is complicated and may overlook faint signals and small variations. With CHIAS IV, the gray values of the chromosome can be readily distinguished by using the pseudocoloration shown with a look-up table (Figure 5-5a).

This image-analysis method provides quantitative and objective identification with improved visibility. An accurate chromosome map can be developed by using the functions available in CHIAS IV (Figure 5-5g). Moreover, automatic averaging of the colorgram profile data for each chromatid of homologous chromosomes can be easily performed. The index-labeling function was devised as a part of the pachytene chromosome analysis of *O. sativa,* and it allowed identification of specific chromosome regions (Chapter 4). The index-labeling function in CHIAS IV can be used to accurately

and easily detect faint, unstable, and small chromatin condensations (FUSCs) [116] and measure the signal peaks that could not be correctly measured in CHIAS III. Thus, image analysis using CHIAS IV has proven to be remarkably effective. The CHIAS IV program along with this analytical procedure protocol can be downloaded from http://www2.kobe-u.ac.jp/~ohmido/index03.htm

5.4.2 Quantitative characteristics of the red clover chromosomes analyzed using CHIAS IV

The heterozygotic locus of the 26S rDNA gene was detected on chromosome 6 of red clover. A homologous chromosome with variant gene loci was slightly larger than its heterozygous counterpart. This difference may be the result of allogamy due to the self-incompatibility caused by the heterozygosity of chromosome 6. Heterozygosis has been reported in the plant chromosomes such as rye and rose [32, 122]. In the present study, I used the HR strain of red clover, since heterozygosis has not been observed in the R130 strain [112].

Complete identification of the red clover chromosome is not possible using only CP or FP data and chromosome lengths and arm ratios in CHIAS IV. However, I successfully employed the FISH method, in which previously obtained probes for rDNA and BAC clones were used, for certain chromosome identification. I believe that a complete chromosome map can be constructed by combining CHIAS IV image analysis and FISH methods, since a signal-position peak would be displayed as a scale along the right side of the idiogram by the index labeling (Figures 5-5f, g).

Thus, CHIAS IV is a powerful tool for the analysis of chromosome images. The chromosome map obtained by CHIAS IV can provide useful information for accurate assembly of genetic markers on the map. Recently, Ohmido *et al.* [121] used CHIAS to develop a quantitative chromosome and linkage map of *L. japonicus*, which is considered a model plant of the Leguminosae family. In the future, a more detailed chromosome map of red clover will be completed by unifying the linkage map and the quantitative chromosome map produced in this study. Furthermore, the use of CHIAS IV will enable the comparative analyses of *L. japonicus* and red clover to determine the

difference between their chromosome maps, thereby proving that this program is a powerful analytical tool for genomic comparison between model and useful crop plants with small chromosomes, such as the plants in the Leguminosae family.

Chapter 6.

Quality evaluation of Christmas Erica using image analysis

6.1 Introduction

Erica formosa is a bush of the Ericaceae Erica genus of South African provenance. *Erica formosa* is a popular pot plant that flowers in early spring. In 2003, the Yamanashi Prefectural Agritechnology Center developed a method of growing the bush so as to allow shipping before the Christmas season when it is in high demand. The bush is trained in the style of a fir tree covered with snow and is known as Christmas Erica [123]. Christmas Erica circulates for a high price, but the upkeep of the quality of the bush is important in maintaining its price in the long term. There is thus a need for an objective quality evaluation standard. In contrast to the case for industrial products, however, it is difficult to qualitatively evaluate the objective appearance of the shape of a breeding plant. The use of image analysis to digitize visual information has rapidly progressed with recent improvements of measuring equipment [124]. Image analysis allows the quality evaluation of *Oryza sativa* (rice) grains [125]. However, there have been few examples of the validation of digitized techniques for the quantitative evaluation of quality in the flower industry. There have been reports of the evaluation of primula and lotus petals, but the evaluation method was employed for plant classification and not evaluation of plant quality [126, 127]. Image analysis of flowers has also been reported for the spray formation of chrysanthemums, but the technique requires an exclusive image processing unit and video camera with an analog signal [45]. There has been no report of the image analysis of *Erica formosa*.

In past analysis of the shape of a plant, a video camera with an analog signal was generally used [44, 125]. This limitation was eliminated by the rapid development of computer technology, and the process of acquiring image information became easy with the combination of a digital camera and personal computer. In the present study, I developed an objective measurement method for the quality evaluation of Christmas Erica through the measurement of the area of the flower using image analysis.

6.2 Materials and Methods

6.2.1 Materials

Erica formosa was cultivated in the Gakuroku branch office (800 m above sea level) of the Yamanashi Prefectural Agritechnology Center. The bushes were being trained as Christmas trees. Bushes in 15-cm-diameter plastic pots were used for region extraction and measurement of the flowering index in April 2003, and bushes in 12-cm-diameter plastic pots were used for a comparison between the flowering index and naked-eye observation in April 2004.

6.2.2 Measurement environment and software

The public-domain software ImageJ (http://rsb.info.nih.gov/ij/) operating on Windows XP was used in the analysis. The image processing command used in the program was developed as a plug-in; *i.e.*, it was an extended command of ImageJ. Eight-bit grayscale images were derived for each channel of the red-green-blue (RGB) photographs to measure the projected area of the shrub outline, and the area of flowers was determined from the gray level.

6.2.3 Digitization of the image

A digital camera (Coolpix2000; Nikon, Tokyo, Japan) was used for the photography. The flowering pot was photographed regularly from the date that the first flower appeared. Photographs were taken from the same direction to compare the change over time. A transmissive photography stand (Photo Cube Pro; inView Co. Ltd., Atsugi, Japan) was used to extract the outline. The height, width and depth of the stand were 900, 900 and 700 mm respectively. A blackboard without luster was set up behind. Each plant photographed with a QPcard 101 (QPcard AB, Helsingborg, Sweden) as a template for the grayscale correction and length. The photographed image was stored in jpeg format (1625 pixels in width by 1024 pixels in height).

6.2.4 Regional extraction

The 24-bit RGB color photography graphics were factored to an 8-bit grayscale image (256 gray levels) of red, green and blue, which are the three primary colors of light. A

median filter was used to reduce noise in each grayscale image. The outline of the plant body is extracted by converting an 8-bit grayscale image into a binarized image in which the dark area is the background and the bright area is the plant body. However, it is difficult to isolate the plant body from the background in the photography image using a uniform threshold. Therefore, a background rejection filter was used for each grayscale image of RGB. The background was then isolated using a threshold. Finally, a binarized image based on the threshold was generated. The extracted area was defined as the projected area of the shape of the bush. Conversion from an RGB color image to grayscale images of each channel and a median filter were employed as in the outline extraction to determine the area of the flower (referred to as the flowering area).

In the binary process, the bright part of a branch is extracted as a line in the flowering area. Therefore, an erode filter and dilate filter were applied to each grayscale image, and a binarized image was created using a threshold.

6.2.5 Flowering index

The flowering regional ratio for the shape of the bush-projected area is referred to as the "flowering index". The calculation is

flowering index = (flowering area / shape of the bush-projected area) × 100.

The flowering area in the outline extraction and the shape of the bush-projected area strongly depend on the naked-eye setting of the threshold. Repeatability was confirmed by photographing 10 pots after flowering. The flowering indexes were measured 10 times for each image.

6.2.6 Evaluation of the measurement value

The flowering index calculated in image analysis was compared with naked-eye evaluation of the same photograph on a computer screen. The index has a value of zero before flowering and a value of 100 for full bloom. Ten pots were photographed four times at regular intervals after the first flower flowering.

6.3 Results

6.3.1 Regional binary extraction

The flowering area and the shape of the bush outline were measured from the 8-bit grayscale images derived from separate channels of the RGB image. As a result, the gray level in green was high in the branch part of *Erica formosa*, but the gray levels in red and blue were low. Figure 6-1 shows the grayscale image extracted from color graphics derived from red (R), green (G) and blue (B). The central right branch of the image can be observed in the grayscale image derived from green clearly. However, it was slightly unclear in the grayscale image derived from red and hardly visible in the grayscale image derived from blue. Graphs in the lower part of Figure 6-1 are density profiles along lines drawn horizontally in the images. Bright areas correspond to high values (8-bit, maximum value of 255) and dark areas to low values (minimum value of zero). In the density profile derived from green, a branch area with a gray level exceeding 100 was detected between pixels 550 and 600, but no such area was observed in the density profiles derived from red and blue. The shape of the bush-projected area could thus only be extracted from the grayscale image derived from green employing the binary process and threshold. Because the background in the photography did not have a flat gray level, it was difficult to extract the background and the shape of the bush from a photograph directly (Figure 6-2 a, b). However, it was confirmed that it was possible to extract the shape of the bush using a background rejection filter (Figure 6-2 c). On the other hand, the grayscale image derived from blue was suitable for the extraction of the white flowering area, because branch regions could not be detected in this image.

Extraction images could be obtained from the shape of the bush-projected area using the green-derived grayscale image and the flowering area using the blue-derived grayscale image (Figure 6-3).

6.3.2 Measurement of the flowering index

For the pot having a diameter of 15 cm, the flowering index was 15 on average on the date of the first flower appearing and 55 on average at full bloom (Figure 6-4). There was high correlation between the flowering index and the number of days since flowering began; high coefficient of determination of $r^2 = 0.988$. In addition, the variation index measured 10 times for the same photographs of the pot just after flowering begun had an average ± standard deviation of 0.030 ± 0.0070. The maximum value was only 0.044. This shows that there was little measurement error when employing the measurement method. There was high positive correlation in the comparison of the flowering index measured by image analysis and evaluation by naked eye; high coefficient of determination of $r^2 = 0.9415$ (Figure 6-5).

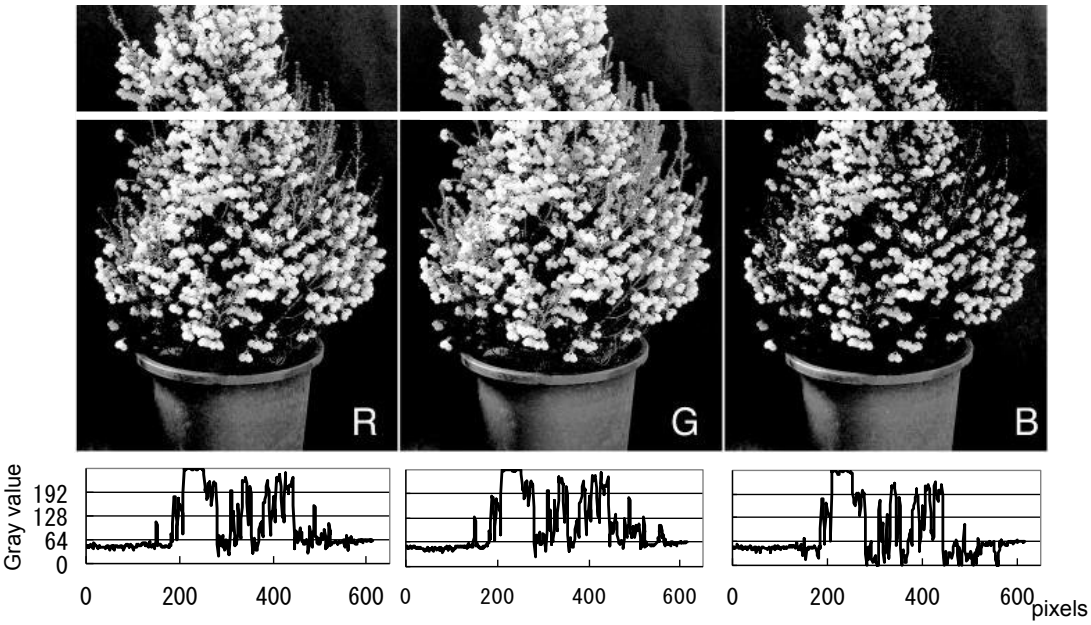

Figure 6-1. RGB-derived grayscale images.

Red-derived (R), green-derived (G) and blue-derived (B) images from left to right. The graphs show the density profiles of the grayscale images on the white lines in the photographs. The gray levels are 8-bit (256 gray levels) from 0 (black) to 255 (white).

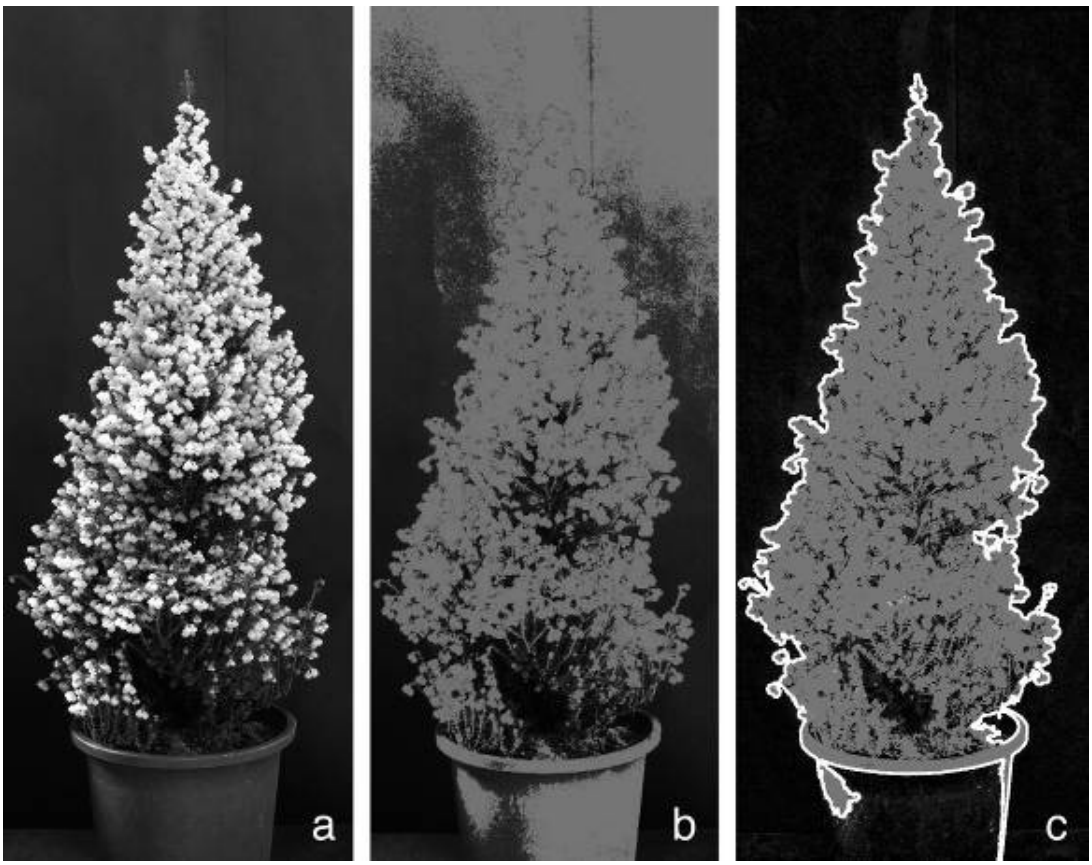

Figure 6-2. Effect of the background rejection filter in background extraction.
a. Photography image.
b. Image extracted without the background rejection filter.
c. Image extracted with the filter.

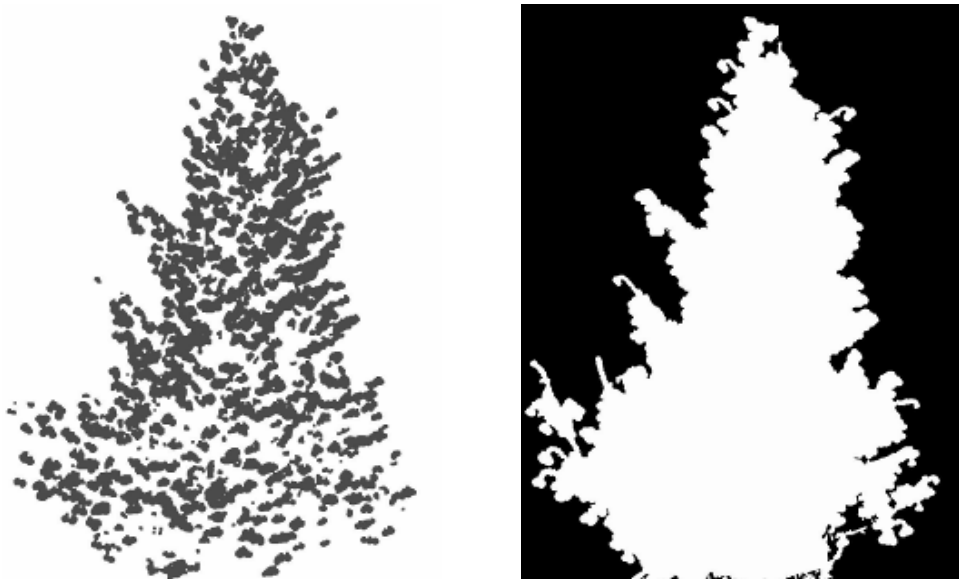

Figure 6-3. Filter-processed binary images for measurement.

The left image shows the flowering area, and the right the bush outline.

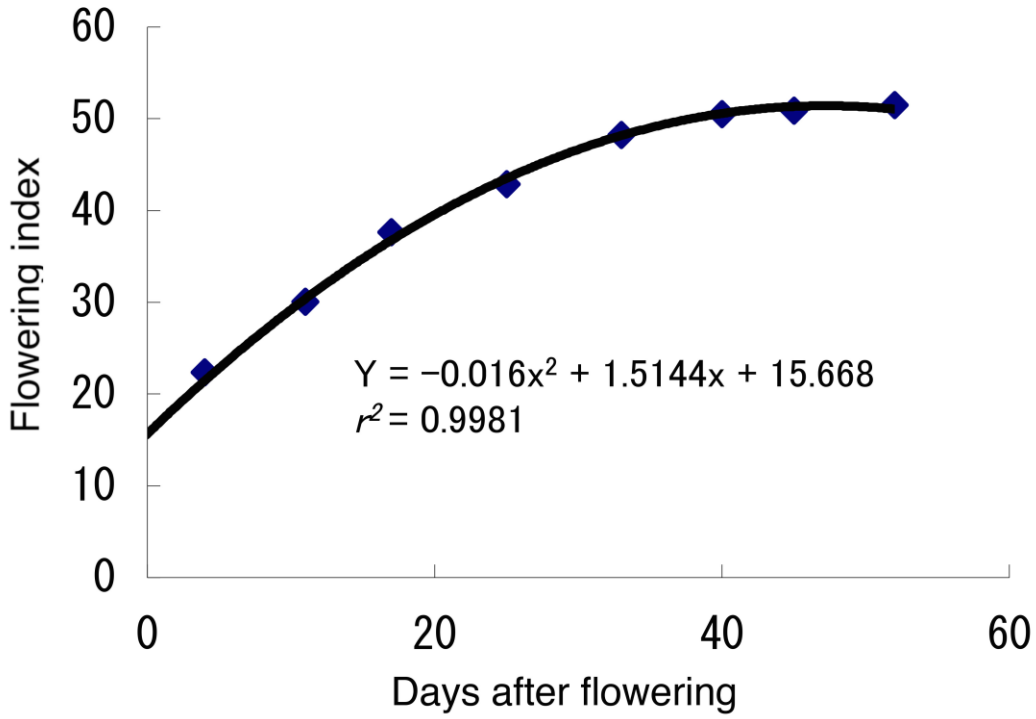

Figure 6-4. Changes in the flowering index of a bush in a 15-cm-diameter pot.

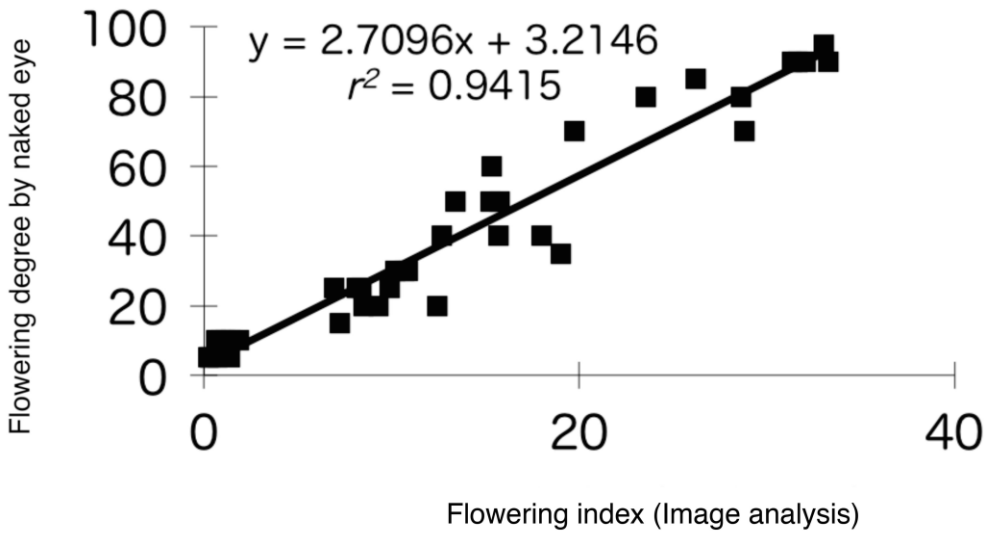

Figure 6-5. Relationship between the flowering degree determined by naked eye and the flowering index for the same photograph.

6.4 Discussion

This chapter presented the quantitative digitizing of flowering in the training of *Erica formosa* through the calculation of a flowering index. The image analysis can evaluate the flower quality of a potted plant, which is difficult to quantify by naked-eye observation. Usually, the shape of a plant does not represent a uniform body, and the flowering degree has not been digitized until now. Dates of first flowering were measured, but did not correspond to the flowering degree determined by naked eye.

Image analysis of such a solid object is usually difficult. It is thought that image analysis is suitable for *Erica formosa* for the following reasons. First, the plant body is trained to be conical by Christmas, and there is little convexo-concave shape. Second, the color phases of a white flower and the green branches and leaves are different. This is clearly seen by converting from an RGB color image to the grayscale of each channel. An outline of the shape of the bush and the areas of white flowers could be extracted from the green-derived image and blue-derived image. Third, there are many (more than 10,000) flowers for a bush in a pot having diameter of 15 cm. The image analysis method presented was effective, whereas measurement by naked eye is virtually impossible.

Primula and lotus flowers have been analyzed using Fourier descriptors [126, 127]. There have also been reports of the analysis of rice seeds and the shape of Glycine max [44, 125]. In these reports, however, plant bodies were broken down for photography. Therefore, such technology is not suitable for shipment evaluation. This chapter presented, in contrast, a method of nondestructive measurement. Christmas Erica was used, in part, because it was easy to move for photography.

In this chapter, a simple transmissive photography stand was used in consideration of photography in greenhouses. There is a reported case of the automation of the threshold used [128, 129], which could be applied to the proposed method by reconsidering the photography system. However, the repeatability of the manual measurement was high; the variation index was only 0.030 on average, indicating little error.

The results of the proposed method were compared with quantification by

naked eye. A plant body was photographed from the same direction to estimate the change in continuous flowering in this chapter. However, it is necessary to measure several pieces of photographs for which the angle is different at the same time to improve reliability. The continuous measurement of flowering described in this chapter can be applied to growth diagnosis and the instruction of cultivation. The image analysis could be applied widely. In the case of Christmas Erica, the image analysis is expected to be applied to the evaluation of branch density. Further application of the evaluation methods to low-cost plants is expected.

The results obtained in this chapter will help on-site agricultural production by improving the quality control and growth diagnosis of *Erica formosa*.

Chapter 7.
General Conclusion

The present study showed the possibility for measurement and evaluation of plants chromosomes and plant shapes using the image analysis method. The development of the chromosome map and the quality of the pot flower were analyzed to achieve this purpose.

First, I developed the image analysis system for plant chromosomes for the universal use. The advantage of this image analysis system is to combine general-purpose input device and personal computer without the usage of an exclusive input device and expensive image processing processor (Chapter 2). Second, I investigated the effectiveness of the quantification by the image analysis method using Gramineae and Fabaceae chromosomes (Chapter 3-5). Third, I developed the lower-cost image analysis method for plant shapes by the use of common digital cameras (Chapter 6).

Image analysis methods were introduced mainly from 1980s to 1990s in various fields of the plant research. It is used widely from the micro-field to the macrofield in the plants studies. In the fundamental research field, as the micro sample, chromosome under the microscopy are analyzed [5]. And, as the macro sample, distribution of the vegetation was analyzed using the remote sensing with the satellite image [6]. However, the image analysis technology was available only to limited researchers, because expensive exclusive image-processing equipments were necessary. The image analysis of the necessary plant chromosome also using an expensive device was limited to the special users in the late 1990s. The image analysis method for a plant chromosome study is composed of functions such as the digitized gray value on the chromosome, the alignment of the chromosome, sorting, pseudo colorization. The development of the chromosome map contribute for the genetic accurate mapping on chromosomes. The third-generation chromosome image analyzing system (CHIAS III) was developed by using an ordinary personal computer with a public domain imaging software, the NIH Image. The effectiveness of the condensation pattern was unequivocally verified by the introduction of an imaging method to characterize the condensation patterns of 12 rice chromosomes [50]. Several quantitative chromosome maps or idiograms based on the condensation pattern have also been developed using

CHIAS I and II [50, 61]. The data obtained using CHIAS III is consistent with those obtained with the chromosome image analyzing systems previously developed. CHIAS III works only with a personal computer without special image processing unit (Chapter 2).

It is important to combine the chromosome image analysis and the fluorescence *in situ* hybridization (FISH) method which labeled fluorescent dyes to genes to proceed with plant chromosome study effectively [21]. Reiterated sequences were positioned on chromosomes with a lot of kinds such as centromeres [8, 9, 22, 23], telomeres [13, 24, 25] and rDNAs [26-32] by FISH. I had proved the possibility for the quantification and the evaluation of the plant by the image analysis method in this study. The image processing is used for a chromosome study frequently including FISH, and the image analysis method becomes the indispensable tool presently.

Genetic maps have been developed in many cultivated plants as tools both for molecular and conventional genetic studies. Generally, however, molecular marker mapping has difficultly and inefficiently proven for polyploid plants. This barrier was reduced in *Saccharum* by the production of haploid *S. spontaneum* [53, 81]. But, prior attempts to karyotype the members of the genus *Saccharum* [88, 89] failed to produce an idiogram to distinguish individual chromosomes. The key element of the present research that made complete identification and characterization of individual *S. sontaneum* chromosomes was the distinctive CP of prometaphase chromosomes using CHIAS III. The 45S and 5S ribosomal RNA gene (rDNA) loci were simultaneously visualized by multi-color fluorescence *in situ* hybridization (McFISH). The simultaneous visualization of two sets of four ribosomal RNA genes confirms tetraploidy of this line. Previously impossible identification of small chromosomes and untestable hypotheses about the polyploid nature of plants can be settled with these two approaches of quantitative karyotyping and FISH (Chapter 3).

For the purpose to improve the resolution of the cytological chromosome map, I developed the image analysis method of the pachytene chromosomes. Pachytene chromosomes have higher resolution than somatic chromosomes, due to their elongated structure in meiosis. In rice, this approach was developed early, and several reports on

pachytene chromosomes were published [94-96] however the results were quite divergent. In the present study, the high-resolution chromosome map with much amount of information was developed. This procedure allows the identification of chromosome 9 from the other rice chromosomes at the pachytene stage by double staining with PI and DAPI. The pachytene map of chromosome 9 consists of twenty-two chromomeres including four chromomeres within the nucleolar organizing region (NOR) and satellite region. It is likely that, by combining the pachytene chromosome map with the linkage map, better understanding between the recombination frequency and the unit-length of a chromosome can be obtained. It represents that the pachytene chromosome map carries important biological information which is not replaced by other maps (Chapter 4).

The usability of the image analysis of chromosomes in foregoing chapters had been shown. I developed the image analysis system of the plant chromosomes which improved human interface for the more researchers to analyze chromosomes. This study had achieved the efficiency by introducing automation processing technology such as sorting or the region extraction into a chromosome image analyzing program. I have demonstrated the effectiveness of image analysis in the allogamous legume, red clover, by using CHIAS IV. In comparison with CHIAS III, CHIAS IV affords improved automation in the analysis procedure. As a result, the analysis time for each chromosome spread was dramatically shortened to approximate one-third of it required using CHIAS III. The new system used ImageJ and multiplatform public-domain image-processing software. CHIAS IV includes the automation of a complicated process and works in most operating system for PC including Windows. The CHIAS IV program along with this procedure protocol can be downloaded from http://www2.kobe-u.ac.jp/~ohmido/index03.htm. The chromosome map obtained by CHIAS IV can provide useful information for accurate assembly of genetic markers on the map. CHIAS IV had accelerated in the progress of the quality of the chromosome map and proved the usefulness of the image analysis in the field of plant. At present, chromosome maps had been developed in many plants using CHIAS III [115, 130-132]. High-resolution pachytene chromosome maps were developed with red clover and *Lotus japonicus*. The visualization is possible not only the genes positioning such as

FISH but also the organization of the chromosome. The visualization technology of histone modification in chromosomes by the immunostaining is developed [37-39]. The image analysis contributes the chromosome analysis which is important tool of biological research. The development of quantitative chromosome map had the correct positional information of connected chromosome conformation (heterochromatin, euchromatin, centromere and nucleolar organizer region) for genomic elucidation, which is now enabled by using the image analysis program developed in this study. In plants such as rice and *Arabidopsis* is which a genome projects were completed[15, 16], cytological chromosome maps using CHIAS were developed [101, 115]. It had been possible that the integration of the genetic information of DNA sequence and linkage maps with cytological quantitative chromosome map improve cytogenetic significance. The integration with chromosome maps and linkage maps is attempted using them [121, 133]. CHIAS IV is downloaded by many international researchers of twelve countries and contributes to plant chromosome analysis widely [134-138]. For example, a kind of the grass having heat stress tolerance, Festulolium hybrid (*Lolium multiflorum* × *Festuca arundinacea*) was analyzed by GISH. The chromosomal characteristics of a single diploid was analyzed by FISH using rDNA probes [138] (Chapter 5).

In the quality evaluation of the plant research, particularly the field of the flower, the objective evaluation was limited to a part of parameters such as length or the weight. The effectiveness of the image analysis was identified as a quality evaluation method of the character that had difficulty in quantification by naked eye observation. Eventually, I had achieved the quality evaluation by the image analysis in the field of the pot flower traits. In *Erica formosa,* there are many (more than 10,000) flowers for a bush in a pot having diameter of 15 cm. It was thought that an image analysis method based on the measurement by the ordinary naked eye was effective. In this study, I applied image processing methods using a personal computer and a general digital camera. As a result, practical system with well user interphase was provided. The program used Java application ImageJ, which was multiplatform public-domain image-processing software as a host application. There was the reported case of the automation of the threshold [128, 129], and the automation of the threshold was

possible by reconsidering a photographing system. The continuous measurement of flowering used in the chapter could be applied to a growth diagnosis and instruction of the cultivation. The image analysis would be applied widely for the plant growth diagnosis and quality managements. A fruit and a leaf can be displayed digitally by applying the automation of a process shown in Chapter 5. It would contribute to shortening of the measuring time (Chapter 6). An image analysis method was applied for the evaluation of flowering degree of Christmas Erica to express more effectively of the plant figures. Although it was not practical to measure the number of the flowers, in the case of Christmas Erica with several thousands of flowers per pot and quantifying area of white flowers became possible. This method for measurement is used in a standard quality for shipment in Yamanashi. When fruit or leaf are photographed, the automation of a process shown in Chapter 5 puts directions together in size order and can display them. And it is thought that these procedures contribute to shortening of the measuring time. Three-dimensional analysis has begun to be used in plant breeding for the phenotype analysis of the root [139]. Moreover, it is expected that the method becomes widely used through the field of any plant study. Using low-cost time-lapse photographing cameras enables growth analysis of plant, it can expect the application to a suitable temperature control to plant.

Practical image analysis technologies were developed in the field of various plant studies such as plant shapes [140, 141] and classification of plants using remote sensing. Development of a forest species classification method [6], the seasonal variation of the evergreen forest [142] and precision grassland management [143] are reported. The future development of an effective application on plant researches using image analysis method is expected.

Chapter 8.

Abstract

I had developed a program for image analyses of plant which worked by personal computer without using an exclusive image processing equipment. Furthermore, I had developed of the chromosome maps and evaluated quality of the pot flower in several kinds of plants using the developed program. The principal results of this study are:

1. The third-generation chromosome image analysing system (CHIAS III) was developed by using an ordinary personal computer with public domain imaging software, the NIH Image. An uneven condensation pattern (CP) appearing on small sugarcane chromosomes at the mitotic prometaphase stage was analyzed and a quantitative chromosome map or idiogram was developed by using CHIAS III.

2. Somatic chromosomes of a wild relative sugarcane (*Saccharum spontaneum L.*) anther culture-derived clone ($2n$=32) were identified and characterized by CHIAS III and molecular cytological methods. The presence of four satellite chromosomes and four nearly identical chromosome sets suggests that the clone is a tetrahaploid with the basic number x=8. A quantitative chromosome map, or idiogram, was developed using image analysis of the condensation pattern (CP) at the prometaphase stage of somatic chromosomes. The simultaneous visualization of the 45S and 5S of four ribosomal RNA genes confirms tetraploidy of this clone.

3. Using rice chromosome 9 as a model, an imaging method to construct a pachytene chromosomal map was developed, by quantifying the fluorescence profile (FP) of each chromomere. The pachytene map of chromosome 9 consists of twenty-two chromomeres including four chromomeres within the nucleolar organizing region (NOR) and satellite region. The pachytene map was compared with the corresponding somatic prometaphase map and the linkage map. The differences among the three maps indicate that each map depicts specific biological information, which is difficult to be substituted by the other maps.

4. An improved chromosome image analyzing system (CHIAS IV) has been released for measurement of the condensation patterns (CPs) in fluorescence images. CHIAS IV is based on ImageJ. A quantitative chromosome map of red clover was produced by combining the qualitative-analysis results obtained using fluorescence *in*

situ hybridization (FISH) mapping with the results of the CHIAS IV image-analysis method.

5. The quality of Christmas Erica, which were trained to a Christmas-tree style on *Erica formosa* and developed were evaluated using image analysis. An objective index for quality evaluation was developed by measuring the area of flowers. After having conversion from an RGB color image to grayscale images of each channel, the flowering index value was calculated by measuring tree shape of a tree outline and the area of flowers from gray levels using ImageJ the multiplatform public-domain image-processing software, which was developed by the National Institutes of Health, US. The result of having compared a flowering index measured by image analysis and evaluation by the naked eye, showed a high correlation. Reliable objectivity from an image analysis was proved by these results.

6. The development of quantitative chromosome map is useful for the elucidation of chromosome conformation in genome research, which is now enabled by developing CHIAS in this study. It had been possible that the integration of the genetic information of DNA sequence and linkage maps with cytological quantitative chromosome map improve cytogenetic significance. Practical image analysis technologies were developed in the field of various plant studies such as plant shapes and classification of plants using remote sensing. The future development of an effective application on plant researches using image analysis method is expected.

Acknowledgments

I wish to express my heartfelt thanks to Professor Dr. Nobuko Ohmido, Kobe University, for her invaluable guidance throughout the study and critical reading of my dissertation. I wish to express my sincere gratitude to Professor Dr. Kiichi Fukui, Osaka University, for his invaluable discussion, continuous encouragement and and guidance about all protocols of the program of CHIAS. I wish to express my sincere gratitude to my director Mr. Kazunori Nakagomi, Yamanashi Prefectural Agritechnology Center, for his invaluable guidance of my dissertation. I grateful thank to Professor Dr. Hideki Ichihashi and Professor Dr. Sumio Yano, Kobe University, for their critical reading and comments. I also grateful thank to Professor Dr. Takuto Koba, Chiba University, for his critical reading and comments.

I am grateful to Drs Paul H. Moore and Sen Ha, Hawaiian Agricultural Research Center for supplying us with the chromosome samples of *S. spontaneum*.

I am very grateful to the members of Chromosome Link for their encouragement. Special thanks go to Dr. Hans J. de Jong, Wageningen University, The Netherlands. Ms. Tomoko Ogihara, National Agricultural Research Center, Hokuriku Research Center, Japan for her technical support in pachytene chromosome preparation, and to Dr. Toshiyuki Wako, National Institute of Agrobiological Sciences, Japan for image analyses on pachytene chromosomes. I am very grateful to Mr. Takao Togawa, Yamanashi Fruit Tree Experiment Station for their valuable cooperation in my experiments. I express my gratitude to the members of the Cold Upland Vegetable and Flower Promotion Center of Yamanashi Prefectural Agritechnology Center, for their technical assistance and heartfelt encouragement.

References

1. Fukui, K. (1990) Utilization of image data for breeding: Image analysis methods in the chromosome research, present and future. *Advances in Breeding (Japan)*

2. Graham, J. and Taylor, C.J. (1980) Automated chromosome analysis using the Magiscan Image Analyser. *Anal. Quant. Cytol.* 2, 237-242

3. Foster, J. (1985) Medical applications of image analysis with the Magiscan 2. *Anal. Quant. Cytol. Histol.* 7, 192-196

4. Rigaut, J.P., Boysen, M., and Reith, A. (1985) Karyometry of pseudostratified, metaplastic and dysplastic nasal epithelium by morphometry and stereology. 2. Automated image analysis (IBAS) of the basal layer of nickel workers. *Pathol. Res. Pract.* 180, 151-160

5. Fukui, K. (1986) Standardization of karyotyping plant chromosomes by a newly developed chromosome image analyzing system (CHIAS). *Theor. Appl. Genet.* 72, 27-32

6. Kawamura, M., Tsujino, K., and Tsujiko, Y. (2005) Development of a Forest Species Classification Method Based on a Decision Tree Method Using High Resolution Satellite Imagery. *Journal of the Japan society of photogrammetry and remote sensing* 44, 54-67

7. Satake, S. and Fukumori, T. (2001) Development of High Performance Color Sorter. *JOURNAL OF THE BREWING SOCIETY OF JAPAN* 96, 688-695

8. Wolfgruber, T.K., Sharma, A., Schneider, K.L., Albert, P.S., Koo, D.H., Shi, J., Gao, Z., Han, F., Lee, H., Xu, R., Allison, J., Birchler, J.A., Jiang, J., Dawe, R.K., and Presting, G.G. (2009) Maize centromere structure and evolution: sequence analysis of centromeres 2 and 5 reveals dynamic Loci shaped primarily by retrotransposons. *PLoS Genet* 5, e1000743

9. Gindullis, F., Desel, C., Galasso, I., and Schmidt, T. (2001) The large-scale organization of the centromeric region in Beta species. *Genome Res.* 11, 253-265

10. Maluszynska, J. and Heslop‐Harrison, J. (1991) Localization of tandemly repeated DMA sequences in Arabidopsis thaliana. *The Plant Journal* 1, 159-166

11. Brandes, A., Thompson, H., Dean, C., and Heslop-Harrison, J.S. (1997) Multiple repetitive DNA sequences in the paracentromeric regions of Arabidopsis thaliana L. *Chromosome Res.* 5, 238-246

12. Richards, E.J. and Ausubel, F.M. (1988) Isolation of a higher eukaryotic telomere from Arabidopsis thaliana. *Cell* 53, 127-136

13. Sykorova, E., Lim, K.Y., Kunicka, Z., Chase, M.W., Bennett, M.D., Fajkus, J., and Leitch, A.R. (2003) Telomere variability in the monocotyledonous plant order Asparagales. *Proceedings. Biological sciences / The Royal Society* 270, 1893-1904

14. Sykorova, E., Lim, K.Y., Chase, M.W., Knapp, S., Leitch, I.J., Leitch, A.R., and Fajkus, J. (2003) The absence of Arabidopsis-type telomeres in Cestrum and closely related genera Vestia and Sessea (Solanaceae): first evidence from eudicots. *The Plant journal* 34, 283-291

15. IRGSP (2005) The map-based sequence of the rice genome. *Nature* 436, 793-800

16. Arabidopsis Genome Initiative (2000) Analysis of the genome sequence of the flowering plant *Arabidopsis thaliana*. *Nature* 408, 796-815

17. Akagi, H. (2000) DNA fingerprinting and variety identification in Japonica rice. *Breeding Research* 2, 89-96

18. Maekawa, M., Kanazawa, A., Tsutsumi, N., Kinoshita, T., Habu, Y., Shiba, H., and Ezura, H. (2013) Epimutagenesis and its application for next generation breeding. *Breeding Research* 15, 42-50

19. Ohsawa, R. (2004) Use of Molecular Markers in Vegetable Breeding. *Horticultural Research (Japan)* 3, 1-6

20. Sato, K. and Fukui, K. (2013) Current status and prospects for education of breeding science. *Breeding Research* 15, 134-138

21. Langer, P.R., Waldrop, A.A., and Ward, D.C. (1981) Enzymatic synthesis of biotin-labeled polynucleotides: novel nucleic acid affinity probes. *Proc. Natl. Acad. Sci. U. S. A.* 78, 6633-6637

22. Heslop-Harrison, J.S., Murata, M., Ogura, Y., Schwarzacher, T., and Motoyoshi, F. (1999) Polymorphisms and genomic organization of repetitive DNA from centromeric regions of Arabidopsis chromosomes. *Plant Cell* 11, 31-42

23. Thompson, H., Schmidt, R., Brandes, A., Heslop-Harrison, J.S., and Dean, C. (1996) A novel repetitive sequence associated with the centromeric regions of Arabidopsis thaliana chromosomes. *Mol. Gen. Genet.* 253, 247-252

24. Ohmido, N. and Fukui, K. (1997) Visual verification of close disposition between a rice A genome-specific DNA sequence (TrsA) and the telomere sequence. *Plant Mol. Biol.* 35, 963-968

25. Schwarzacher, T. and Heslop-Harrison, J. (1991) In situ hybridization to plant telomeres using synthetic oligomers. *Genome* 34, 317-323

26. Fukui, K., Kamisugi, Y., and Sakai, F. (1994) Physical mapping of 5S rDNA loci by direct cloned biotinylated probes in barley chromosomes. *Genome* 37, 105-111

27. Kamm, A., Galasso, I., Schmidt, T., and Heslop-Harrison, J. (1995) Analysis of a repetitive DNA family from Arabidopsis arenosa and relationships between Arabidopsis species. *Plant Mol. Biol.* 27, 853-862

28. Kitamura, S., Inoue, M., Ohmido, N., and Fukui, K. (2000) Quantitative chromosome maps and rDNA localization in the T subgenome of N*icotiana tabacum* L.

and its putative progenitors. *Theor. Appl. Genet.* 101, 1180-1188

29. Maluszynska, J. and Heslop-Harrison, J. (1993) Molecular cytogenetics of the genus Arabidopsis: in situ localization of rDNA sites, chromosome numbers and diversity in centromeric heterochromatin. *Ann. Bot.* 71, 479-484

30. Mukai, Y., Endo, T., and Gill, B. (1991) Physical mapping of the 18S. 26S rRNA multigene family in common wheat: identification of a new locus. *Chromosoma* 100, 71-78

31. Ohmido, N., Kijima, K., Akiyama, Y., de Jong, J.H., and Fukui, K. (2000) Quantification of total genomic DNA and selected repetitive sequences reveals concurrent changes in different DNA families in indica and japonica rice. *Mol. Gen. Genet.* 263, 388-394

32. Akasaka, M., Ueda, Y., and Koba, T. (2002) Karyotype analyses of five wild rose species belonging to septet A by fluorescence *in situ* hybridization. *Chromosome Science* 6, 17-26

33. Hennig, L., Taranto, P., Walser, M., Schonrock, N., and Gruissem, W. (2003) Arabidopsis MSI1 is required for epigenetic maintenance of reproductive development. *Development* 130, 2555-2565

34. Kumpatla, S.P. and Hall, T.C. (1998) Recurrent onset of epigenetic silencing in rice harboring a multi-copy transgene. *The Plant journal* 14, 129-135

35. Stokes, T.L., Kunkel, B.N., and Richards, E.J. (2002) Epigenetic variation in Arabidopsis disease resistance. *Genes Dev.* 16, 171-182

36. Yin, B.L., Guo, L., Zhang, D.F., Terzaghi, W., Wang, X.F., Liu, T.T., He, H., Cheng, Z.K., and Deng, X.W. (2008) Integration of cytological features with molecular and epigenetic properties of rice chromosome 4. *Mol Plant* 1, 816-829

37. Fuchs, J., Demidov, D., Houben, A., and Schubert, I. (2006) Chromosomal histone

modification patterns--from conservation to diversity. *Trends Plant Sci* 11, 199-208

38. Ramsahoye, B.H., Biniszkiewicz, D., Lyko, F., Clark, V., Bird, A.P., and Jaenisch, R. (2000) Non-CpG methylation is prevalent in embryonic stem cells and may be mediated by DNA methyltransferase 3a. *Proc. Natl. Acad. Sci. U. S. A.* 97, 5237-5242

39. Wako, T., Fukuda, M., Furushima-Shimogawara, R., Belyaev, N.D., Turner, B.M., and Fukui, K. (1998) Comparative analysis of topographic distribution of acetylated histone H4 by using confocal microscopy and a deconvolution system. *Anal. Chim. Acta* 365, 9-17

40. Sumner, A.T., Evans, H.J., and Buckland, R. (1971) New technique for distinguishing between human chromosomes. *Nature (Lond.) New Biology* 232, 31–32

41. Caspersson, T., Lomakka, G., and Møller, A. (1971) Computerized chromosome identification by aid of the quinacrine mustard fluorescence technique. *Hereditas* 67, 103-109

42. Zahed, L., Murer-Orlando, M., and Bobrow, M. (1989) The application of automated metaphase scanning to direct preparations of chorionic villi. *Prenat. Diagn.* 9, 7-17

43. Ninomiya, S. (1990) Utilization of image data for breeding: Analysis of binary image and its application. *Advances in Breeding (Japan)*

44. Ninomiya, S. and Shigemori, I. (1991) Quantitative evaluation of soybean (*Glycine max* L. Merrill) plant shape by image analysis. *Japan. J. Breed* 41, 485-497

45. Kai, K., Kondo, N., Hayashi, T., Shibano, Y., Konishi, K., and Monta, M. (1995) Studies on algorithm for evaluating spray formation of cut chrysanthemum [*Dendranthema* x *grandiflorum*], 2: Investigation of the evaluation index using image processing. *Environment Control in Biology* 33

46. Omori, H. and Iwata, H. (1998) Development of Image Analysis Software,

BioImage ver.1, for Windows to Measure Leaf Area. *Agricultural Information Research* 7, 71-80

47. Fukui, K. (1995) Quantitative chromosome map as a basis of biosciences. In *Kew Chromosome Conference IV*. (Brandham, P.E. and Bennett, M.D., eds), pp. 201-213, The Royal Botanic Gardens

48. Fukui, K. (1996) Plant chromosomes at mitosis. In *Plant Chromosomes: Laboratory Methods.* (Fukui, K. and Nakayama, S., eds), pp. 1-18, CRC Press

49. Hu, C.H. (1964) Further studies on the chromosome morphology of *Oryza sativa* L. In *Rice genetics and cytogenetics*, pp. 51-61, Elsevier Publishing Company

50. Fukui, K. and Iijima, K. (1991) Somatic chromosome map of rice by imaging methods. *Theor. Appl. Genet.* 81, 589-596

51. Kamisugi, Y., Furuya, N., Iijima, K., and Fukui, K. (1993) Computer-aided automatic identification of rice chromosomes by image parameters. *Chromosome Res.* 1, 189-196

52. Fukui, K. and Nakayama, S. (1996) Analysis of chromosome information. In *Plant Chromosomes: Laboratory Methods.* (Fukui, K. and Nakayama, S., eds), pp. 247-261, CRC Press

53. Fitch, M.M. and Moore, P.H. (1983) Haploid production from anther culture of *Saccharum spontaneum* L. *Z Pflanzenphysiol* 109, 197-206

54. Kato, S., Hirose, T., Akiyama, Y., O'neill, C.M., and Fukui, K. (1997) Manual on the chromosome image analyzing system III, CHIAS III. *Res. Report Hokuriku Natl. Agr. Exp. Stn.* 36, 1-76

55. Nakayama, S. and Fukui, K. (1997) Quantitative chromosome mapping of small plant chromosomes by improved imaging on CHIAS II. *Genes Genet. Syst.* 72, 35-40

56. Carlson, L., Caspersson, T., Foley, G.E., Kudynowski, J., Lomakka, G., Simonsson, E., and Soren, L. (1963) The application of quantitative cytochemical techniques to the study of individual mammalian chormosomes. *Exp. Cell Res.* 31, 589-594

57. Mendelsohn, M.L., Conway, T.J., Hungerford, D.A., Kolman, W.A., Perry, B.H., and Prewitt, J.M.S. (1966) Computer-oriented analysis of human chromosomes. 1. Photometric estimation of DNA content. *Cytogenet* 5, 223-242

58. Granlund, G.H. (1973) The use of distribution functions to describe integrated density profiles of human chromosomes. *J Theor Biol* 40, 573-589

59. Granum, E. and Lundsteen, C. (1979) Description of chromosome banding patterns by band transition sequences. *Clin Genet* 15, 418-429

60. Lundsteen, C. and Piper, J. (1989) *Automation of Cytogenetics.* Springer-Verlag

61. Fukui, K., Nakayama, S., Ohmido, N., Yoshiaki, H., and Yamabe, M. (1998) Quantitative karyotyping of three diploid Brassica species by imaging methods and localization of 45s rDNA loci on the identified chromosomes. *Theor. Appl. Genet.* 96, 325-330

62. Kurata, N. and Omura, T. (1978) Karyotype analysis in rice I. A new method for identifying all chromosome pairs. *Jpn J Genet* 53, 251-255

63. Stebbins, G.L. (1950) In *Variation and Evolution in Plants*, pp. 300, Columbia University Press

64. Swanson, C.P. (1957) Polyploidy and evolution. In *Cytology and Cytogenetics*, pp. 500-517, Prentice-Hall Inc.

65. Gould, F.W. (1968) In *Grass Systematics*, pp. 2, McGraw Hill

66. Sreenivasan, T.V., Ahloowalia, B.S., and Heinz, D.J. (1987) Cytogenetics. In *Sugarcane Improvement through Breeding* (Heinz, D.J., ed), pp. 211-253, Elsevier

67. Whalen, M.D. (1991) Taxomomy of *Saccharum* (Poaceae). *Baileya* 23, 109-125

68. Panje, R.R. and Babu, C.N. (1960) Studies in *Saccharum spontaneum* distribution and geographical association of chromosome numbers. *Cytologia* 25, 152-172

69. Parthasarathy, N. (1948) Origin of noble sugar-canes (*Saccharum officinarum* L.). *Nature* 161, 608

70. Raghavan, T.S. (1951) The sugarcanes of India: Some cytogenetical considerations. *J. Hered.* 42, 199-206

71. Darlington, C.D. and Janaki-Ammal, E.K. (1945) Chromosome atlas of flowering plants., pp. 421-422, Allen & Unwin Ltd.

72. Bremer, G. (1961) Problems in breeding and cytology of sugarcane. *Euphytica* 10, 59-78

73. Grivet, L., D'Hont, A., Roques, D., Feldmann, P., Lanaud, C., and Glaszmann, J.C. (1996) RFLP mapping in cultivated sugarcane (*Saccharum* spp.): genome organization in a highly polyploid and aneuploid interspecific hybrid. *Genetics* 142, 987-1000

74. Fukui, K. and Kakeda, K. (1990) Quantitative karyotyping of barley chromosomes by image analysis methods. *Genome* 33, 450-458

75. Fukui, K. and Kamisugi, Y. (1995) Mapping of C-banded *Crepis* chromosomes by imaging methods. *Chromosome Res.* 3, 79-86

76. D'Hont, A., Rao, P., Feldmann, P., Grivet, L., Islam-Faridi, N., Taylor, P., and Glaszmann, J.C. (1995) Identification and characterisation of intergenric hybrids, *S. officinarum* X *Erianthus arundinaceus*, with molecular markers and *in situ* hybridization. *Theor. Appl. Genet.* 91, 320-326

77. D'Hont, A., Ison, D., Alix, K., Roux, C., and Glaszmann, J.C. (1998) Determination of basic chromosome numbers in the genus *Saccharum* by physical mapping of

ribosomal RNA genes. *Genome* 41, 221-225

78. D'Hont, A., Grivet, L., Feldmann, P., Rao, S., Berding, N., and Glaszmann, J.C. (1996) Characterisation of the double genome structure of modern sugarcane cultivars (*Saccharum* spp.) by molecular cytogenetics. *Mol. Gen. Genet.* 250, 405-413

79. Ohmido, N. and Fukui, K. (1995) Cytological studies of African cultivated rice, *Oryza glaberrima*. *Theor. Appl. Genet.* 91, 212-217

80. Takaiwa, F., Oono, K., and Sugiura, M. (1984) The complete nucleotide sequence of a rice 17s rRNA gene. *Nucl Acids Res* 12, 5441-5448

81. Moore, P.H. and Fitch, M.M. (1990) Sugarcane (*Saccharum* spp.) anther culture studies. *Biotech Agr Forest* 12, 480-497

82. Wu, K.K., Burnquist, W., Sorrells, M.E., Tew, T.L., Moore, P.H., and Tanksley, S.D. (1992) The detection and estimation of linkage in polyploids using single-dose restriction fragments. *Theor. Appl. Genet.* 83, 294-300

83. Da Silva, J.A.G., Sorrells, M.E., Burnquist, W.L., and Tanksley, S.D. (1993) RFLP linkage map and genome analysis of Saccharum spontaneum. *Genome* 36, 782-791

84. Al Janabi, S.M., Honeycutt, R.J., McClelland, M., and Sobral, B.W.S. (1993) A genetic linkage map of *Saccharum spontaneum* L. "SES 208.". *Genetics* 134, 1249-1260

85. Da Silva, J.A.G., Honeycutt, R.J., Burnquist, W.L., Al Janabi, S.M., Sorrells, M.E., Tanksley, S.D., and Sobral, B.W.S. (1995) *Saccharum spontaneum*. L. SES 208 genetic map combing RFLP and PCR-based markers. *Mol Breed* 1, 165-179

86. Stevenson, G.C. (1965) In *Genetics and Breeding of Sugarcane*, pp. 163-212, Longmans

87. Ohmido, N., Akiyama, Y., and Fukui, K. (1998) Physical mapping of unique

nucleotide sequences on identified rice chromosomes. *Plant Mol. Biol.* 38, 1043-1052

88. Nair, M.K. (1972) Cytogenetics of *Saccharum*. III. Karyotype analysis and meiosis in *S. spontaneum*. *Nucleus* 15, 107-117

89. Sreenivasan, T.V. (1975) Cytogenetical studies in *Saccharum spontaneum*. *Proc Ind Acad Sci* 81B, 131-144

90. Fransz, P.F., Armstrong, S., Jong, J.H.d., Parnell, L.D., Drunen, C.V., Dean, C., Zabel, P., Bisseling, T., and Jones, G.H. (2000) Integrated cytogenetic map of chromosome arm 4S of *A. thaliana*: structural organization of heterochromatic knob and centromere region. *Cell* 100, 367-376

91. Rick, C.M. and Barton, D.W. (1954) Cytological and genetical identification of the primary trisomics of the tomato. *Genetics* 39, 640-666

92. Ross, K.J., Fransz, P., and Jones, G.H. (1996) A light microscopic atlas of meiosis in *Arabidopsis thaliana*. *Chromosome Res.* 4, 507-516

93. Havekes, F.W., de Jong, J.H., Heyting, C., and Ramanna, M.S. (1994) Synapsis and chiasma formation in four meiotic mutants of tomato (*Lycopersicon esculentum*). *Chromosome Res.* 2, 315-325

94. Shastry, S.V.S., Rangao, R.D.R., and Misra, R.N. (1960) Pachytene analysis in Oryza-I. Chromosome morphology in *Oryza sativa*. *Indian J. Genet. Plant Breed.* 20, 15-21

95. Kurata, N., Omura, T., and Iwata, N. (1981) Studies on centromere, chromomere and nucleolus in pachytene nuclei of rice, *Oriyza sativa*, microsporocytes. *Cytorogia* 46, 791-800

96. Khush, G.S., Singh, R.J., Sur, S.C., and Librojo, A.L. (1984) Primary trisomics of rice: Origin, morphology, cytology and use in linkage mapping. *Genetics* 107, 141-163

97. Cheng, Z., Buell, C.R., Wing, R.A., Gu, M., and Jiang, J. (2001) Toward a cytological characterization of the rice genome. *Genome Res.* 11, 2133-2141

98. Fukui, K. and Mukai, Y. (1988) Condensation pattern as a new image parameter for identification of small chromosomes in plants. *Jpn. J. Genet.* 63, 359-366

99. Ohmido, N., Kijima, K., Ashikawa, I., de Jong, J.H., and Fukui, K. (2001) Visualization of the terminal structure of rice chromosomes 6 and 12 with multicolor FISH to chromosomes and extended DNA fibers. *Plant Mol. Biol.* 47, 413-421

100. Sano, Y. and Sano, R. (1990) Variation of the intergenic spacer region of ribosomal DNA in cultivated and wild rice species. *Genome Res.* 33, 209-218

101. Iijima, K., Kakeda, K., and Fukui, K. (1991) Identification and characterization of somatic rice chromosomes by imaging methods. *Theor. Appl. Genet.* 81

102. Fukui, K. (1996) Advances in rice chromosome research, 1990-95. In *Rice Genetics III, Proc. 3rd Intl. Rice Genet. Symp.* (Khush, G.S., ed), pp. 117-130., Rice Res. Inst.

103. Lorite, P., Aránega, A.E., Luque, F., and Palomeque, T. (1997) Analysis of the nucleoar organizing regions in the ant *Tapinoma nigerrimum* (Hymenoptera, Formicidae). *Heredity* 78, 578-582

104. Takaiwa, F., Kikuchi, S., and Oono, K. (1990) The complete nucleotide sequence of the intergenic spacer between 25S and 17S rDNAs in rice. *Plant Mol. Biol.* 15, 933-935

105. Dawe, R.K., Sedat, J.W., Agard, D.A., and Cande, W.Z. (1994) Meiotic chromosome pairing in maize is associated with a novel chromatin organizaiton. *Cell* 76, 901-912

106. Peterson, D.G., Lapitan, N.L.V., and Stack, M.S. (1999) Localization of single- and low-copy sequences on tomato synaptonemal complex spreads using fluorescence

in situ hybridization (FISH). *Genetics* 152, 427-439

107. Cheng, Z., Presting, G.G., Buell, C.R., Wing, R.A., and Jiang, J. (2001) High-resolution pachytene chromosome mapping of bacterial artificial chromosomes anchored by genetic markers reveals the centromere location and the distribution of genetic recombination along chromosome 10 of rice. *Genetics* 157, 1749-1757

108. Gustafson, J.P., Butler, E., and McIntyre, C.L. (1990) Physical mapping of a low-copy DNA sequence in rye (*Secale cereale* L.). *Proc Natl. Acad. Sci. USA* 87, 1899-1902

109. Künzel, G., Korzun, L., and Meister, A. (2000) Cytologically integrated physical restriction fragment length polymorphism maps for the barley genome based on translocation breakpoints. *Genetics* 154, 397-412

110. Sato, S. and Tabata, S. (2006) *Lotus japonicus* as a platform for legume research. *Curr. Opin. Plant Biol.* 9, 128-132

111. Isobe, S., Klimenko, I., Ivashuta, S., Gau, M., and Kozlov, N.N. (2003) First RFLP linkage map of red clover (*Trifolium pratense* L.) based on cDNA probes and its transferability to other red clover germplasm. *Theor. Appl. Genet.* 108, 105-112

112. Sato, S., Isobe, S., Asamizu, E., Ohmido, N., Kataoka, R., Nakamura, Y., Kaneko, T., Sakurai, N., Okumura, K., Klimenko, I., Sasamoto, S., Wada, T., Watanabe, A., Kohara, M., Fujishiro, T., and Tabata, S. (2005) Comprehensive structural analysis of the genome of red clover (*Trifolium pratense* L.). *DNA Res.* 12, 301-364

113. Kamisugi, Y. and Fukui, K. (1990) Automatic karyotyping of plant chromosomes by imaging techniques. *Biotechniques* 8, 290-295

114. Akiyama, Y., Kato, S., and Fukui, K. (2004) Image analysis as a tool for molecular cytology. *Recent Research Developments in Genetics & Breeding.* 1, 385-396

115. Ito, M., Ohmido, N., Akiyama, Y., and Fukui, K. (2000) Quantitative chromosome

map of *Arabidopsis thaliana* L. by imaging methods. *Cytologia* 65, 325-331

116. Ito, M., Miyamoto, J., Mori, Y., Fujimoto, S., Uchiumi, T., Abe, M., Suzuki, A., Tabata, S., and Fukui, K. (2000) Genome and chromosome dimensions of *Lotus japonicus*. *J. Plant Res.* 113, 435-442

117. Abramhoff, M.D., Magelhaes, P.J., and Ram, S.J. (2004) Image processing with ImageJ. *Biophotonics International* 11, 36-42

118. Otsu, N. (1979) Threshold selection method from gray-level histograms. *IEEE Trans. Syst. Man Cybern.* 9, 62-66

119. Fukui, K. (2005) Recent development of image analysis methods in plant chromosome research. *Cytogenet. Genome Res.* 109, 83-89

120. Ohmido, N., Sato, S., Tabata, S., and Fukui, K. (2007) Chromosome maps of legumes. *Chromosome Res.* 15, 97-103

121. Ohmido, N., Ishimaru, A., Kato, S., Sato, S., Tabata, S., Hayashi, M., and Fukui, K. (2010) Integration of cytogenetic and genetic linkage maps of *Lotus japonicus*, a model plant for the legume. *Chromosome Res.* 18, 287-299

122. Nagaki, K., Tsujimoto, H., and Sasakuma, T. (1999) A novel repetitive sequence, termed the JNK repeat family, located on an extra heterochromatic region of chromosome 2R of Japanese rye. *Chromosome Res.* 7, 95-101

123. Togawa, T. and Kato, S. (2007) Development of growing method for training to Christmas-tree style on *Erica formosa*. *Bulletin of the Yamanashi Prefectural Agricultural Technology Center* 1, 9-14

124. Akiyama, Y. and Kato, S. (2000) Advances in image analysis. *kagakutoseibutu* 38, 466-471

125. Akiyama, Y., Yamada, H., Takahara, Y., and Yamamoto, K. (1997) Comparison of

standard images of longitudinal sections and transverse sections for evaluation of white-core in rice kernel for sake brewery. *Japanese Journal of Breeding* 47, 379-384

126. Zheng, Z., Iwata, H., Ninomiya, S., and Tamura, Y. (2005) Quantitative evaluation of partial shape characteristics of petals of the sacred lotus based on P-type Fourier descriptors. *Breed Res* 7, 133-142

127. Yoshioka, Y., Iwata, H., Ohsawa, R., and Ninomiya, S. (2004) Analysis of petal shape variation of *Primula sieboldii* by elliptic fourier descriptors and principal component analysis. *Ann Bot* 94, 657-664

128. Hayashi, T., Sato, T., Sakai, K., Iwata, T., Oida, T., Mawaki, M., Saio, K., Ninomiya, S., and Yoshida, T. (1993) Diagnostic approach to the growth of paddy rice [Oryza sativa] using image analysis, 1: Estimation of leaf area index by rate of vegetation coverage. *Bulletin of the Fukui Agricultural Experiment Station* 30, 9-18

129. Otsu, N. (1980) An automatic threshold selection method based on discriminant and least squares criteria. *IEICE TRANSACTIONS on Information and Systems (Japanese Edition)* 63, 349-356

130. Apisitwanich, S., Shishido, R., Akiyama, Y., and Fukui, K. (2000) Quantitative chromosome map of a representative indica rice. *Euphytica* 116, 161-166

131. Ito, M., Ohmido, N., Akiyama, Y., Fukui, K., and Koba, T. (2000) Characterization of spinach chromosomes by condensation patterns and physical mapping of 5S and 45S rDNAs by FISH. *J. Am. Soc. Hort. Sci.* 125, 59-62

132. Goel, S., Chen, Z., Conner, J.A., Akiyama, Y., Hanna, W.W., and Ozias-Akins, P. (2003) Delineation by fluorescence in situ hybridization of a single hemizygous chromosomal region associated with aposporous embryo sac formation in Pennisetum squamulatum and Cenchrus ciliaris. *Genetics* 163, 1069-1082

133. Kataoka, R., Hara, M., Kato, S., Isobe, S., Sato, S., Tabata, S., and Ohmido, N.

(2012) Integration of linkage and chromosome maps of red clover (*Trifolium pratense* L.). *Cytogenet. Genome Res.* 137, 60-69

134. Ohmido, N., Shimoura, A., Kato, S., Isobe, S., and Tabata, S. (2013) Kudzu (*Pueraria lobata* Ohwi) karyotyping using FISH and Chromosome Image Analysis System IV. *Chromosome Science* 16, 17-21

135. Young, H.A., Sarath, G., and Tobias, C.M. (2012) Karyotype variation is indicative of subgenomic and ecotypic differentiation in switchgrass. *BMC Plant Biol.* 12, 117

136. Grosso, V., Farina, A., Gennaro, A., Giorgi, D., and Lucretti, S. (2012) Flow sorting and molecular cytogenetic identification of individual chromosomes of *Dasypyrum villosum* L. (*H. villosa*) by a single DNA probe. *PLoS One* 7, e50151

137. Giorgi, D., Pandozy, G., Farina, A., Grosso, V., Lucretti, S., Crinò, P., and Saccardo, F. (2012) Karyotype of Globe Artichoke (*Cynara cardunculus var. scolymus)*: Preliminary Studies to Define Its Chromosome Morphology. In *VIII International Symposium on Artichoke, Cardoon and their Wild Relatives 983*, pp. 133-138

138. Akiyama, Y., Kimura, K., Yamada-Akiyama, H., Kubota, A., Takahara, Y., and Ueyama, Y. (2012) Genomic characteristics of a diploid F_4 festulolium hybrid (Lolium multiflorum x Festuca arundinacea). *Genome* 55, 599-603

139. Clark, R.T., MacCurdy, R.B., Jung, J.K., Shaff, J.E., McCouch, S.R., Aneshansley, D.J., and Kochian, L.V. (2011) Three-dimensional root phenotyping with a novel imaging and software platform. *Plant Physiol.* 156, 455-465

140. Tanabata, T., Yamada, T., Shimizu, Y., Shinozaki, Y., Kanekatsu, M., and Takano, M. (2010) Development of automatic segmentation software for efficient measurement of area on the digital images of plant organs. *Hort. Res. (Japan)* 9, 501-506

141. Shono, H., Serizawa, K., Yamaguchi, K., Ushikusa, T., Matsushima, U., Koide, S., Tatsuzawa, F., and Takeda, J. (2012) A new method with a pair of polarizing filters for quantification of luster of corollas of Japanese gentian flowers for determination of growth stage. *Agricultural Information Research* 21, 95-105

142. Tanigaki, Y., Harada, I., Sekiyama, A., and Hara, K. (2012) Characteristics and Seasonal variations in reflectance of evergreen forest including Madake and Mousouchiku bamboo determined by using ALOS/AVNIR-2. *Journal of the Japan society of photogrammetry and remote sensing* 50, 361-366

143. Kawamura, K. and Akiyama, T. (2012) Remote Sensing for Precision Grassland Management. *Journal of The Remote Sensing Society of Japan* 32, 232-244